Structure-activity relationship of serotonin derived tocopherol lipids

Venkanna Muripiti, Thasneem Yoosuf Mujahid, Venkata Harsha Vardhan Boddeda, Shrish Tiwari, Srujan Kumar Marepally, Srilakshmi V Patri, Vijaya Gopal

PII: S0378-5173(18)30815-9
DOI: https://doi.org/10.1016/j.ijpharm.2018.10.072
Reference: IJP 17890

To appear in: *International Journal of Pharmaceutics*

Received Date: 11 July 2018
Revised Date: 24 October 2018
Accepted Date: 29 October 2018

Please cite this article as: V. Muripiti, T.Y. Mujahid, V.H.V. Boddeda, S. Tiwari, S.K. Marepally, S.V. Patri, V. Gopal, Structure-activity relationship of serotonin derived tocopherol lipids, *International Journal of Pharmaceutics* (2018), doi: https://doi.org/10.1016/j.ijpharm.2018.10.072

Structure-activity relationship of serotonin derived tocopherol lipids

Venkanna Muripiti[a], Thasneem Yoosuf Mujahid[b], Venkata Harsha Vardhan Boddeda[b], Shrish Tiwari, Srujan Kumar Marepally[c], Srilakshmi V Patri*[a], Vijaya Gopal*[b],

[a]National Institute of Technology, Warangal-506004, Telangana, India

[b]CSIR-Centre for Cellular and Molecular Biology, Uppal Road, Hyderabad-500007, Telangana, India.

[c]Center for Stem Cell Research (CSCR), Christian Medical College Campus, Bagayam, Vellore-632002, TN, India

* Corresponding authors

Vijaya Gopal: E-mail: vg562000@gmail.com

P. V. Srilakshmi; E-mail: patrisrilakshmi@nitw.ac.in

Abstract

Tocopherol-based lipids are widely used for nucleic acid delivery. Using tocopherol molecules, we designed and synthesized 5-HT functionalized lipids by tethering 5-hydroxytryptamine (5-HT), a small molecule ligand as the head group to a natural amphiphilic molecule namely α-tocopherol (Vitamin E). This is with the aim of delivering nucleic acids specifically into cells expressing the serotonin receptors (5-hydroxytryptamine[5-HT]) which are abundant in the central nervous system. In order to achieve target recognition, we adopted an approach wherein two structurally different lipid molecules having serotonin as the head group was conjugated to tocopherol via different linkers thus generating lipids with either free -NH_2 or -OH moiety. The corresponding lipids designated as **Lipid A** (Tocopheryl carbonate serotonin-NH_2) and **Lipid B** (Tocopheryl 2-hydroxy propyl ammonium serotonin-OH), were formulated with co-lipids 1,2-dioleoyl-sn-glycero-3-phosphatidyl-ethanolamine (DOPE) and 1,2-dioleoyl-sn-glycero-sn-3-phosphatidylcholine (DOPC) and evaluated for their ability to deliver plasmid DNA through reporter gene expression assays *in vitro*. Furthermore, the physicochemical characteristics and cellular interactions of the formulations were examined using serotonin-receptor enriched cells in order to distinguish the structural and functional attributes of both lipids. Cell-based gene expression studies reveal that in comparison to **Lipid A**, a formulation of **Lipid B** prepared with DOPE as the co-lipid, contributes to efficient uptake leading to significant enhancement in transfection. Specific interactions explored by molecular docking studies suggests the role of the hydroxyl moiety and the enantiospecific significance of serotonin- conjugated tocopherol lipids in recognizing these receptors thus signifying a promising lipid-based approach to target the serotonin receptors in the central nervous system.

Keywords: Serotonin, Tocopherol, Gene Delivery, 5-Hydroxytryptamine receptors (5-HT), Targeted Delivery

Introduction

In the context of gene therapy, non-viral nucleic acid delivery is a viable alternative for the intervention of various human diseases [1-3]. The approach mainly utilizes cationic lipid formulations, engineered nanoparticles or peptides and their derivatives for delivering DNA *in vitro* and *in vivo* [4-7]. Among these, cationic lipid-based vectors have contributed to the diversity and repertoire of gene delivery vehicles and have been widely used for nucleic acid therapy and clinical applications [8-11]. Essentially, these approaches facilitate targeted delivery of plasmid DNA in a cell-specific and non-toxic manner while simultaneously increasing the therapeutic efficacy. Selective targeting of the liposome/pDNA (+/-) complexes may be achieved through the incorporation of cell specific ligands on the liposomal surface through direct formulation or by covalent coupling [10-12]. In order to fully realize the therapeutic potential, the delivery vehicle must protect the genetic material or nucleic acid against nucleases in serum-rich biological milieu to enable selective transport to the targeted tissues while fostering up take and consequential endosomal escape[13]. Although cationic vectors can mediate effective gene transfer, tissue specific delivery *in vivo* is still a major hurdle. Till date, tissue-specific targeting of cationic liposome/DNA (+/-) has been accomplished primarily by two different methods. The first approach involves transfection of selected tissues, such as nasal epithelium, neuronal, arterial endothelium, lung, or tumors following local delivery of lipid-based complexes to distinct regions. This straight forward approach has led to its early success in the clinic[14] for the intervention of several diseases that include cystic fibrosis and cancer. The second approach entails target selectivity by coupling cell- binding ligands to enhance cell selectivity. Examples include, conjugation of serotonin targeting 5-HT receptor[15-17] transferrin [18] or carbohydrates [19] to liposomes for the purpose of complementing the intrinsic activities of lipids with ligands that can target a specific receptor.

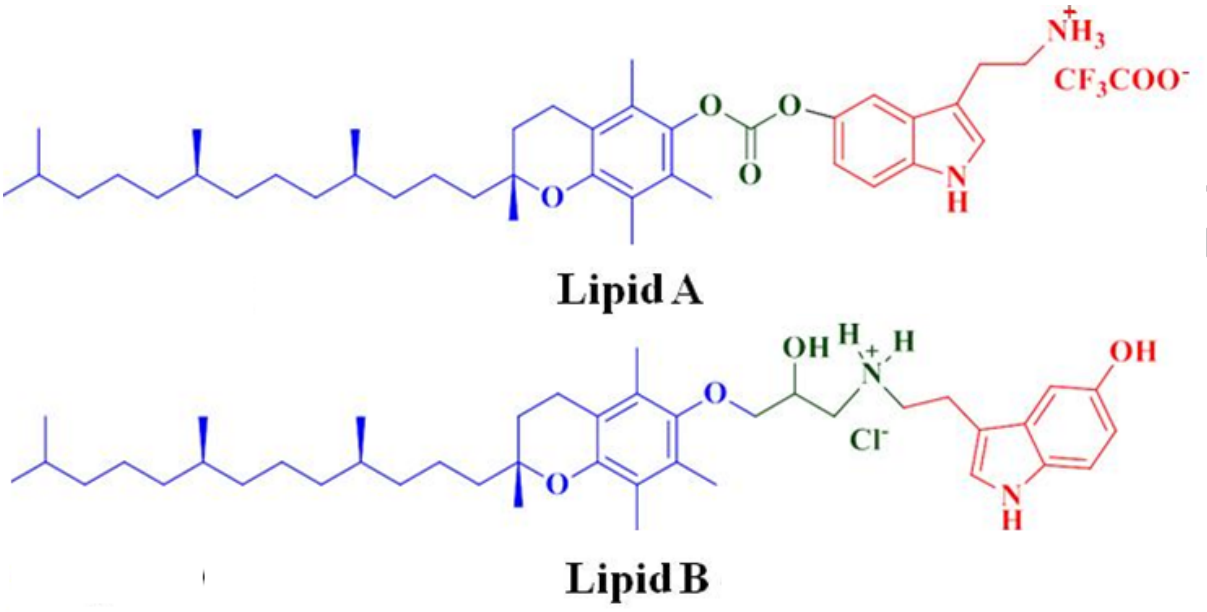

Figure.1. Chemical structures of serotonin-based cationic lipids

Receptors for serotonin (5-hydroxytryptamine [5-HT] as neuro transmitters are abundant in neural as well as non-neural tissues. Serotonin is an important member of the GPCR (G-protein coupled receptors) superfamily acts as a neuro transmitter and is involved in the etiology of large number of neuro degenerative diseases. Dizeyi et al has confirmed the over expression of 5-HT receptors in prostate cancer tissues through ligand binding assays [20, 21]. Recent studies have shown the involvement of serotonin in the peripheral tissues. These non-pharmacological functions have been linked to its chemical properties through receptor-independent mechanisms [22] with potent antioxidant properties. Besides, the antioxidative properties of α-tocopherol has been demonstrated [23-25] and the molecule has been used in treating ROS (reactive oxygen species) related diseases[26].

Serotonin possesses two reactive functional groups i.e. phenolic hydroxyl and primary amine. Through mutagenesis studies, Ho et al., established the involvement of hydroxyl and amine groups indirect receptor binding through interaction with serine, aspartate and threonine residues present in different transmembrane helices of the receptor. Importantly, mutational

and modeling studies reveal that serotonin receptor prefers ligands with a hydrogen bond accept or at a position corresponding to the hydroxyl group in serotonin. In this study, we explored the potential of the hybrid conjugate to enhance DNA delivery to 5-HT receptor-enriched cells. This is with the anticipation that serotonin upon conjugation to α-tocopherol through the reactive groups will retain the combined properties and at the same time reduce the toxicity while increasing cell viability upon transfection. We covalently linked serotonin to α-tocopherol through the reactive -NH_2 and -OH groups and characterized the molecules by examining the structure-activity relationship (SAR) arising from subtle differences in lipid architecture. This is with the premise that the structure may influence transfection efficiency and which was examined through functional and computational studies. To the best of our knowledge, this is the first study reporting the synthesis and use of 5-HT-derived tocopherol lipid as a unique non-toxic conjugate for nucleic acid delivery specifically into cells that express the serotonin receptor.

Results &Discussion

Chemical characterization of serotonin conjugates

To examine structure-based activity and functionality of serotonin derived tocopherol lipids, two cationic **Lipids A (-NH2)** and **Lipid B (-OH)** (**Schemes 1 & 2**) were designed and synthesized. Design in **Lipid A** depicts the conjugation of α-tocopherol to serotonin, through a carbonate linker at –OH group of 5-HT ligand, while **Lipid B** was prepared by conjugating 5-HT to tocopheryl glycidyl ether through a β-hydroxy linker at –NH group of 5-HT ligand. While **Lipid A** was synthesized by the coupling of tocopheryl chloroformate with Boc-protected serotonin, followed by deprotection of the intermediate compound with trifluoro acetic acid (**Scheme 1**), **Lipid B** (**Scheme 2**) (α-tocopherylglycidyl ether) in triethylamine at -10 to 0 ˚C for ~12 h followed by quaternization using HCl in dry methanol. The structures of

all the intermediates (**Scheme 1**) were confirmed by both ^{1}H NMR and mass spectral analysis. The purity of the final conjugates was confirmed by High Resolution Mass Spectrometry (HRMS) and analytical High Performance Liquid Chromatography (HPLC) methods. ^{1}H NMR spectra of all the intermediates **I-V** (**Scheme1**), ^{1}HNMR and HRMS-mass spectra of the final **Lipid A** and **Lipid B** and the HPLC chromatograms for the final conjugates **Lipid A** (**-NH_2**) and **Lipid B (-OH)** in two different mobile phases (100% methanol and 95:5 methanol/water v/v) ,are depicted in **Figures S1-S12** of the Supporting Information.

Scheme 1

Synthesis of Lipid A

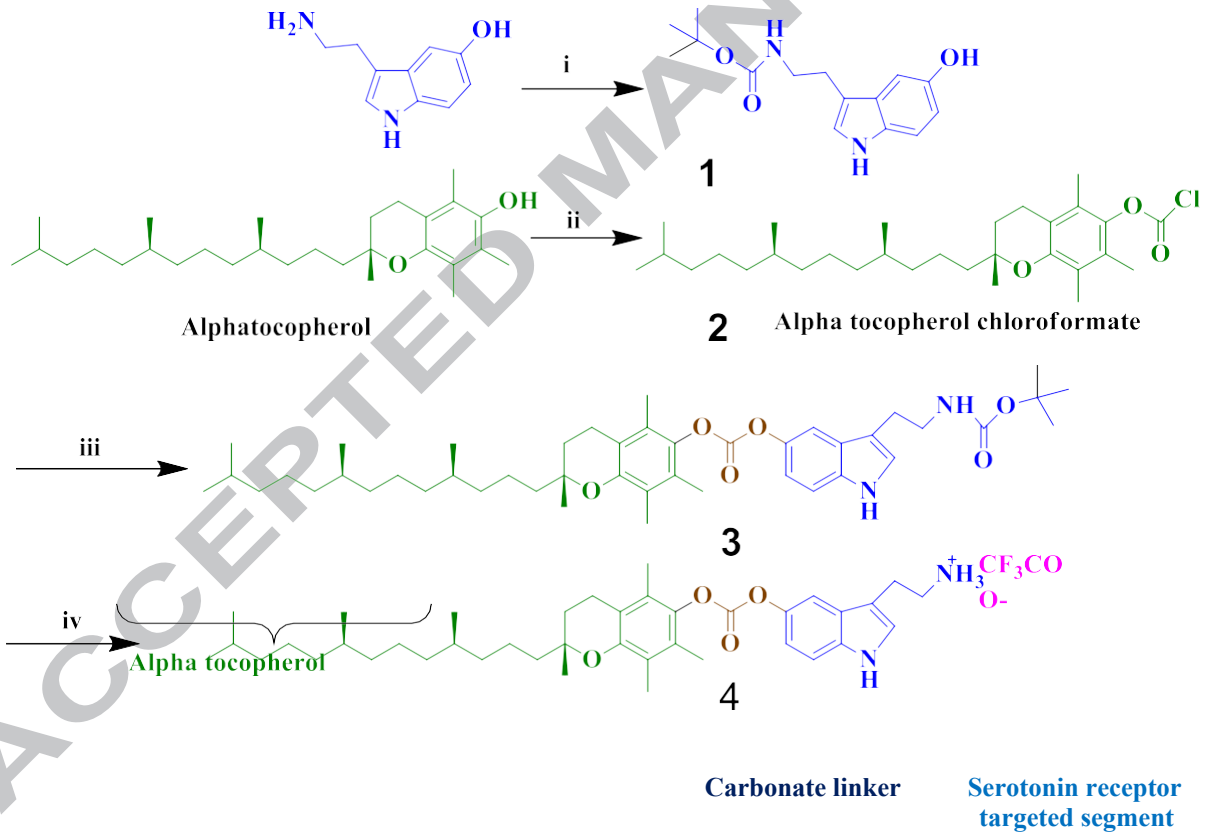

Reagents: i) Dry DCM, Et_3N, BOC_2O, 12 h RT ii) Dry THF, Et_3N, Diphosgene, 12 h RT iii) Boc serotonin, dry DCM, 12 h RT iv) dry DCM, CF_3COOH, 12 h RT

Scheme 2

Synthesis of Lipid B

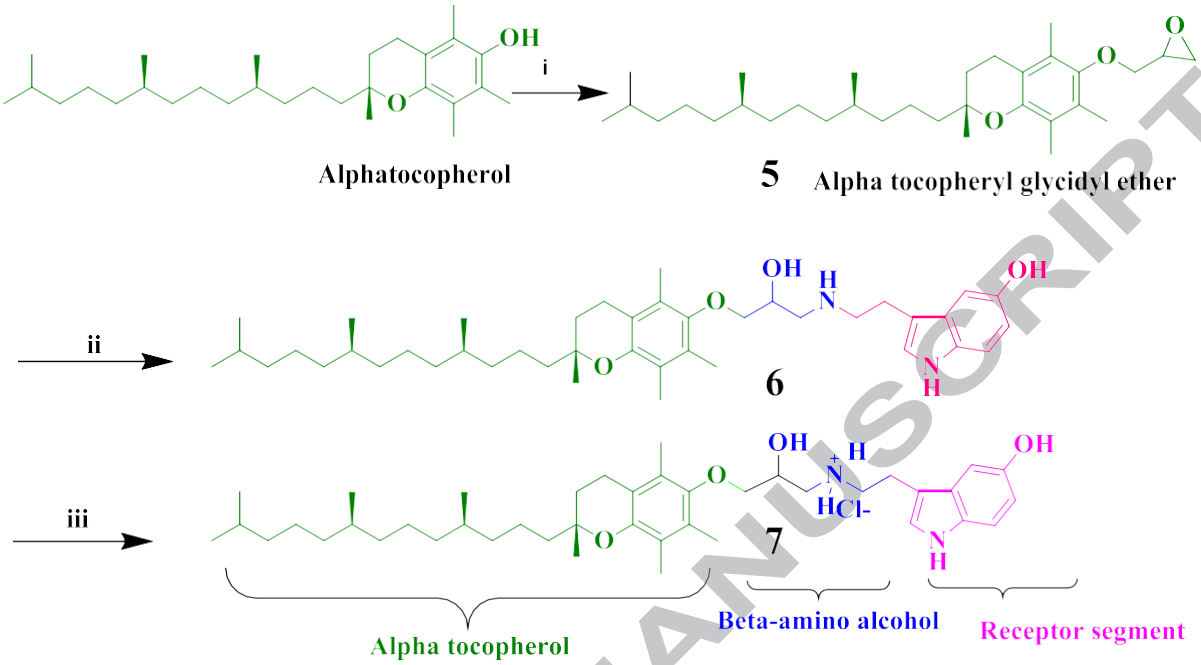

Reagents: i) Epichlorohydrin, 50% KOH solution, tetra butyl ammonium hydrogen sulphate ($Bu_4N^+HSO_4$) and 5 h RT ii) Serotonin, -10°C, Et_3N, 12 h RT iii) Dry MeOH in HCl, 12 h RT

Preparation of Liposomes

Cationic liposomes were prepared with **Lipid A** (**-NH_2**) and **Lipid B (-OH)** by the dry lipid film hydration method as described[27] at varying molar ratios (0.5:1, 1:1 and 2:1) and formulated with co-lipids DOPC and DOPE. Following thin film preparation and drying, lipids were hydrated in sterile water (or buffer at pH 7.4) and subsequently sonicated at room temperature for ~6 min. All the formulations i.e. **Lipid A: DOPE, Lipid A: DOPC, Lipid B: DOPE** and **Lipid B: DOPC** were observed to form stable uniform liposomal suspensions at 2:1 molar ratio. No precipitation was observed for 8 weeks following storage at 4°C.

DNA binding ability of Lipid A and Lipid

To evaluate the extent of DNA binding, **Lipid A** and **Lipid B** formulated with co-lipids **DOPE** and **DOPC** were complexed with plasmid DNA and evaluated through agarose gel electrophoresis and heparin binding assays. Following electrophoresis, binding was observed at very low charge ratio of 1:1 in the case **Lipid A: DOPE, Lipid B: DOPE, Lipid A: DOPC** and **Lipid B: DOPC**. It was also observed that ~ >90% of plasmid DNA was bound at 2:1 and 4:1 N/P charge ratios. Complete binding of DNA was achieved at 8:1 N/P charge ratio (**Figure 2A**) as seen by the retention of the lipoplexes in the well, indicating net neutrality of lipoplexes at the higher charge ratio. This was further supported by surface potential measurement of lipoplexes, **Figure 2B**, which indicates neutralization of negatively charged DNA upon the addition of cationic liposomal conjugates. **Lipid A: DOPE, Lipid B: DOPE, Lipid A: DOPC** and **Lipid B: DOPC** were positive at low charge ratio of 1:1 (5-9 mV). Further increase was observed at 8:1 charge ratio (28-30 mV) (**Figure 2B**). To further elucidate the strength of binding and stability, lipoplexes were treated with heparin, an anionic mucopolysaccharide, which competes with negatively charged DNA (**Figure 2B)**. As observed, binding efficiency of all the formulations were found to be similar (**Figure 2B**) even in the presence of heparin, indicating strong liposome-DNA interactions that are unaffected in the presence of heparin. The stability of the lipoplexes may also be attributed to the favorable hydrogen-bonding interactions between DNA and quaternary amine and hydroxyl functionalities present in the polar head group region of **Lipid A** and **Lipid B** respectively**.** Together these studies reveal that the formulations possess suitable attributes at 2:1 lipid/DNA charge ratios and hence considered optimal for *in vitro* DNA delivery applications.

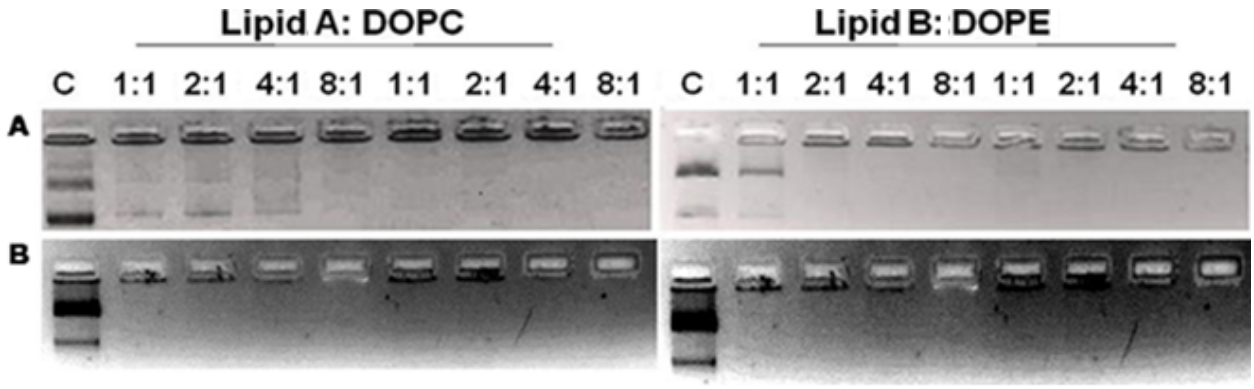

Figure 2. Interaction of Lipid A and Lipid B formulations with DNA: Electrophoretic migration pattern of **Lipid A** and **Lipid B** formulated with co-lipid DOPC (left panel) and DOPE (right panel) in the absence **(**top panel) and presence of heparin (bottom panel) at the indicated charge ratios. Details of the experiment are as described in the text.

Characterization of lipoplexes

As gene delivery is governed by parameters such as surface charge and size, we analyzed these aspects by measuring the zeta potential and hydrodynamic diameter through dynamic light scattering (DLS). Lipoplexes prepared with **Lipid A** and **Lipid B** formulated with DOPE or DOPC were in the size range of 180-190 nm. In comparison, formulations prepared with DOPC were 850-950 nm. These results suggest that the co-lipid may have an effect on the liposome dimension (**Figure 3A**). Lipoplexes with DOPE as the co-lipid were 400-800 nm in dimension at all charge ratios of (1:1-8:1). In contrast, formulations with DOPC were larger, measuring between 450-1250 nm. It was observed that this kinetic increase in lipoplex size at increasing lipid concentration may be due to polyanion induced aggregation [28-30]. The resultant increase at higher charge ratios may also possibly be due to the dilution of lipoplexes in bicarbonate ion enriched media during incubation [31, 32]. Moreover, formulations of both **Lipid A** and **Lipid B**, at 2:1 charge ratios were < 500 nm, a dimension that may enhance uptake. Interestingly, at 2:1 charge ratio, both lipids formulated with DOPE were <300 nm. Surface charge of lipoplexes prepared with **Lipid A** and **Lipid B** (N/P) also measured, **Figure 3A**. Free cationic liposomes have a surface potential of <40 mV and all the lipoplexes at the charge

ratios tested (1:1 to 4:1) have a positive surface potential below 32 mV. At 8:1 charge ratios, all four lipoplexes displayed a surface potential of >35 mV, which suggests increase in the rate of condensation of DNA and positive surface charge upon lipid binding and as a function of charge ratio. Interestingly, the surface potential at 2:1 charge ratio measured < 9mV.

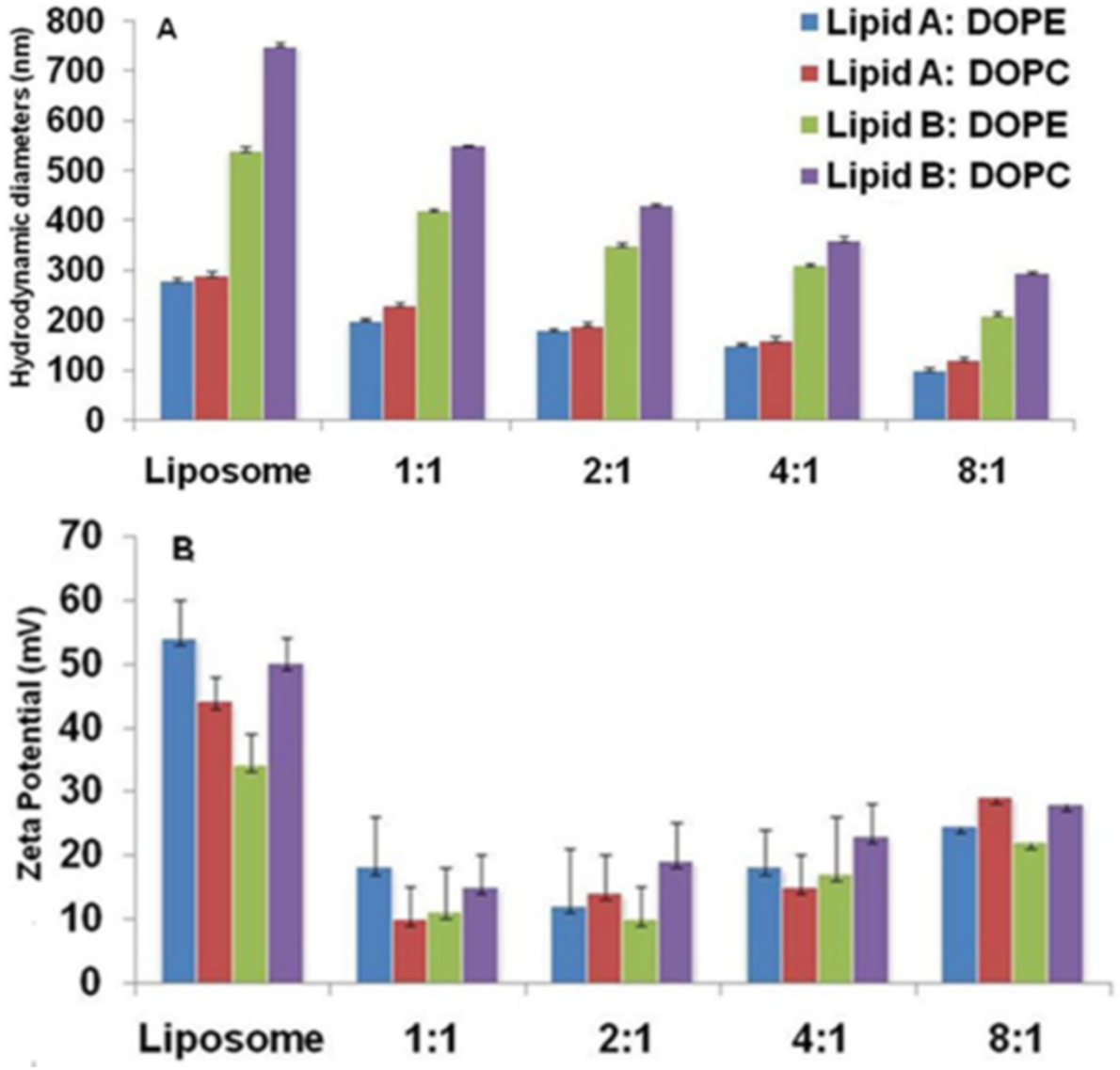

Figure 3. Hydrodynamic diameter (**A**) & Zeta Potential (ξ, mV) (**B**) of **Lipid A** and **Lipid B** formulated with DOPE or DOPC. Lipoplexes were prepared in DMEM (without serum) at the indicated charge ratios. Data represents mean ±SD n=3). Statistical analysis was performed by Two-way ANOVA.

Transient transfection: Target specificity of serotonin conjugates

We investigated the cell specificity and transfection potential of serotonin-α-tocopherol hybrid conjugate formulations through reporter gene expression assays using HEK-293T, Neuro-2a, and HepG2 cells **(Figure 4A)**. Cells were treated with lipoplexes that were prepared using **Lipid A** and **Lipid B** formulated with DOPE and DOPC using plasmid pCMVβ-gal DNA at charge ratios of 2:1 and 4:1, with Lipofectamine as the benchmark standard. Enhanced activity was observed at charge ratio 2:1 than at 4:1 with both formulations with DOPE as the co-lipid, (**Figure 4A**). Lipids formulated with DOPE were observed to be far more efficient than their DOPC counterparts. This may be due to smaller size of lipoplexes prepared with DOPE than DOPC. Moreover, when compared to **Lipid A**, **Lipid B** showed greater activity in all cells except HEK293T. Comparing the structures of **Lipid A** and **B**, the longer linker plus the exposed hydroxyl moiety of **Lipid B** may evoke synergistic interactions as well as enantiospecific interactions with the DNA and cell membrane receptor for providing higher transfection rates. It was also observed that among HEK293T, HepG2 and Neuro2a, the transfection efficiency mediated by both lipids in HEK293T cells was maximal when lipids were formulated with DOPE. Moreover, compared to Lipofectamine 3000, both formulations showed higher transfection efficiency in HEK293T at 2:1 charge ratio. To further gain insight into the target specificity to 5-HT receptor, transfection assays were performed using T-CHO cells which express the serotonin receptors (5-HT_{1A}R) [33]. For comparison and as control, CHO cells were identically transfected in parallel. It was observed that both the lipids showed higher transfection efficiency when formulated with DOPE than with DOPC (**Figure 4B**) as seen from enhanced reporter gene expression, which reiterates the role of auxiliary lipid DOPE in influencing the morphology and size of lipoplexes and subsequent internalization of nucleic acids. It was earlier observed that formulations that included serotonin lipid-conjugates mediated selective uptake of plasmid DNA in TCHO cells stably expressing serotonin receptors than CHO [34, 35]. Subsequent experiments (**Figure 4A**) further confirmed the target ability

of **Lipid A** and **Lipid B** which delineates that formulations of both the lipids demonstrate greater activity in T-CHO compared to CHO, due to higher (~14 times) greater receptor density in T-CHO cell lines [35], Moreover, transfection mediated by lipoplexes prepared with **Lipid B**: DOPE exhibited ~2- 2.5-fold higher activity in T-CHO and lipoplexes prepared with **Lipid A**:DOPE showed 1.5-2 fold higher efficacy compared to control (**Figure 4A**). Specific and efficient uptake of lipoplexes into CHO-5-HT_{1A}R cells, were also conclusively demonstrated by flow cytometry studies (**Figure7**). Collectively, our results suggest the increased uptake of lipoplexes may have led to enhanced reporter gene expression specifically in TCHO cells, hence following the overall rank order **Lipid B: DOPE** > **Lipid A: DOPE** > **Lipid B**: **DOPC** > **Lipid A: DOPC** in mediating target-selectivity. The differential transfection potential of **Lipid A** and **B** indicate that the chemical structure of serotonin conjugate head group and linker length plays an important role in determining. The higher activity of **Lipid B** possibly denotes better hydrogen bonding of the exposed hydroxyl terminal of **Lipid B** in contrast to the N-H amide bonds of **Lipid A** and this promotes favorable head group conformation at specific binding sites on serotonin receptor to invoke higher vesicle internalization as well as transfection in serotonin receptor-enriched cells.

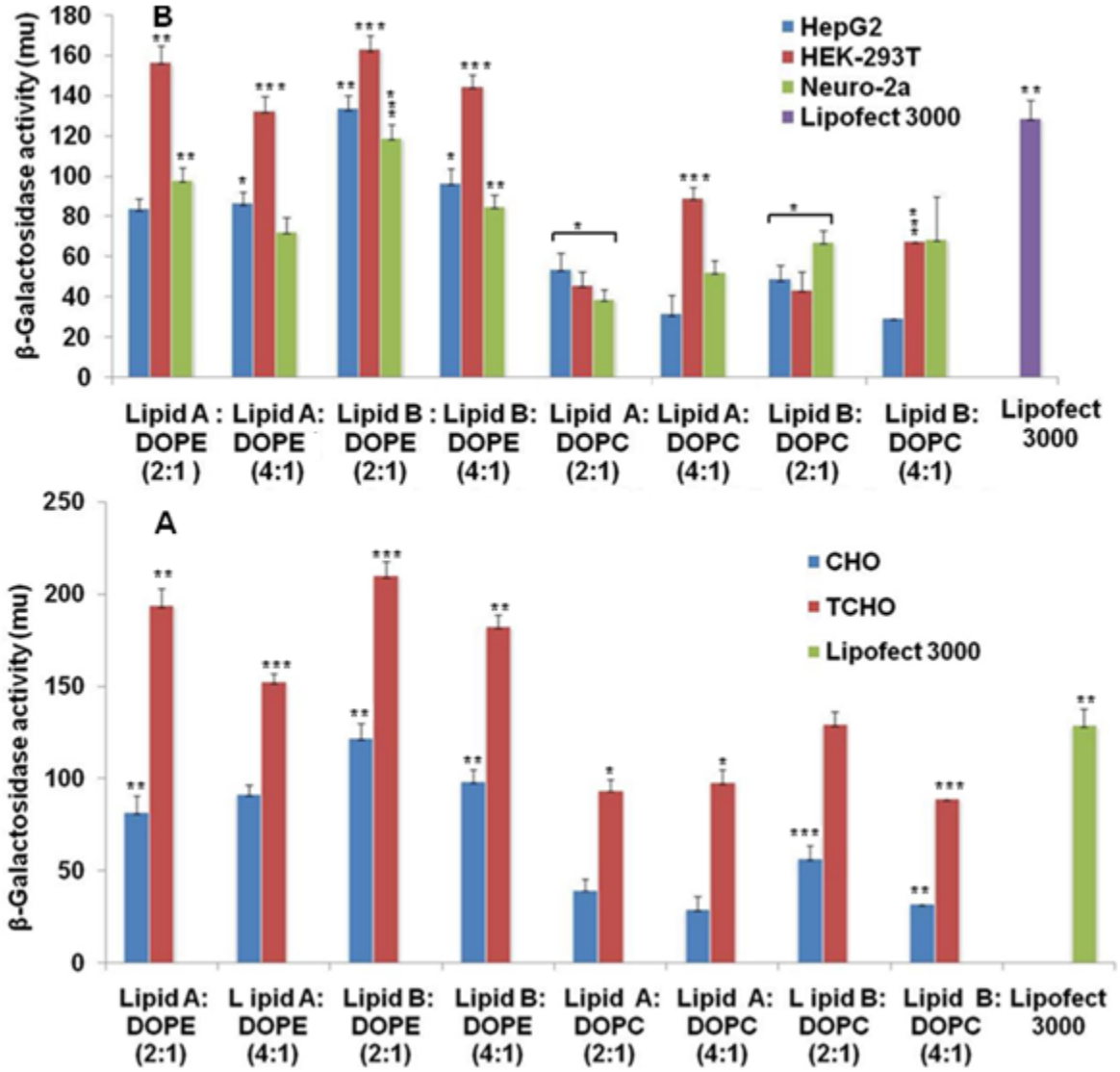

Figure 4. Transient transfection in vitro: TCHO, HepG2, CHO, Neuro-2a and HEK-293T cells were treated with **Lipid A** and **Lipid B** formulated with DOPE/DOPC using pCMVβ-Gal in the absence of serum. Statistical analysis was performed by Two-way ANOVA (*P<0.05, **P<0.01,***P<0.001).

Transfection was also evaluated using pEGFP plasmid as the reporter gene encoding green fluorescence protein in HEK-293T and HepG2 cells using four formulations. (**Figure 5-6**) Following an incubation period of 48 h, cells were visualized by fluorescence microscopy and quantitated. Analysis of GFP expression revealed the superior efficiency of **Lipid B: DOPE** compared to **Lipid A: DOPC** or **Lipid B: DOPC** and Lipofectamine, which in line with our aforesaid observations (**Figure 5 & 6**).

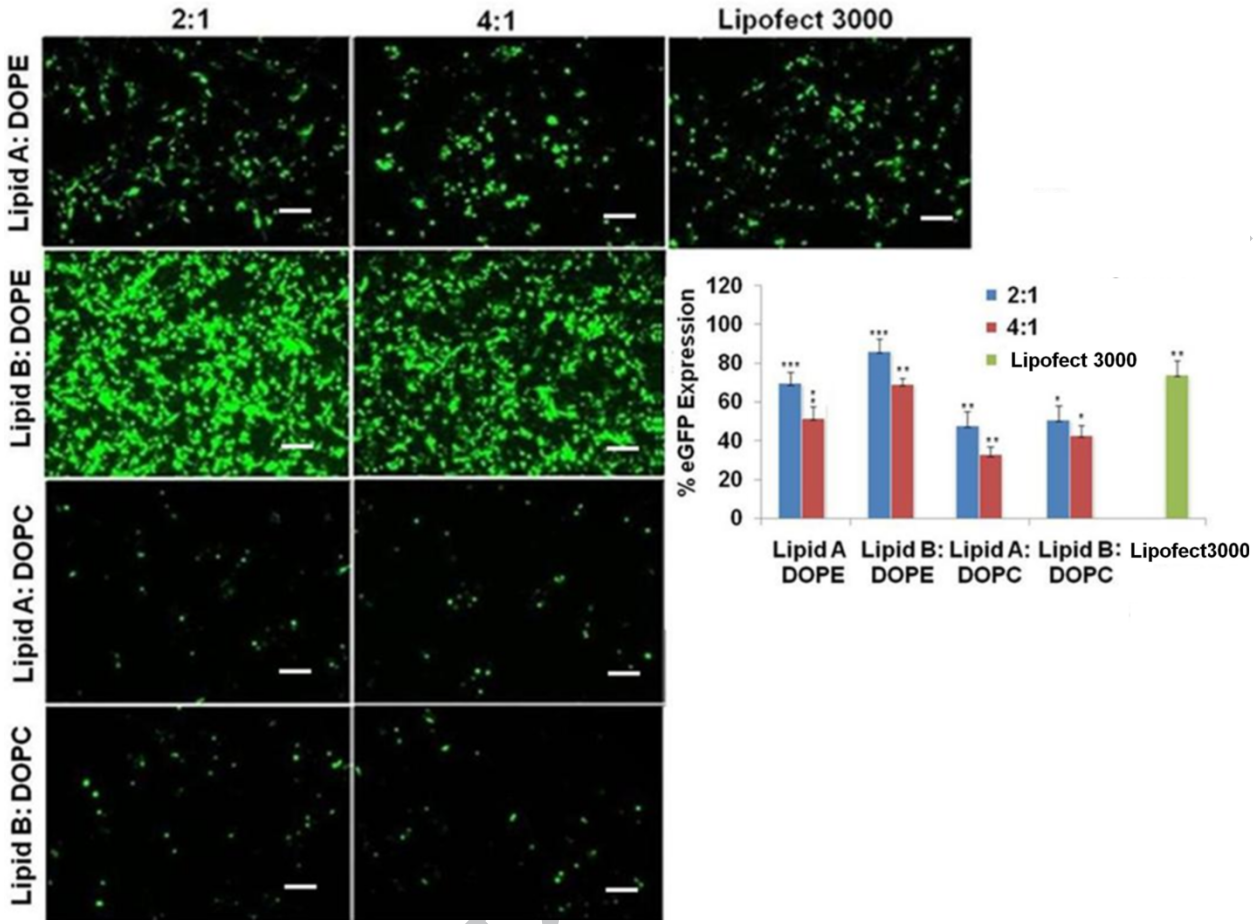

Figure 5. Tr**ansfection in HEK-293T cells**. A) Images depict GFP fluorescence following transfection mediated by **Lipid A** and **Lipid B** formulations at charge ratios 2:1 and 4:1.Lipoplexes were prepared and incubated with HEK-293T cell lines for 4 h in presence of 10% serum subsequently replaced with complete medium and images acquired by fluorescence Microscopy48hposttransfectionB) Representative graph depicts the transfection efficiencies in terms of percentage GFP positive cells. Statistical analysis was performed by Two-way ANOVA (*P<0.005, **P<0.01, ***P<0.001)(Magnification/scale Bars = 100 µm.)

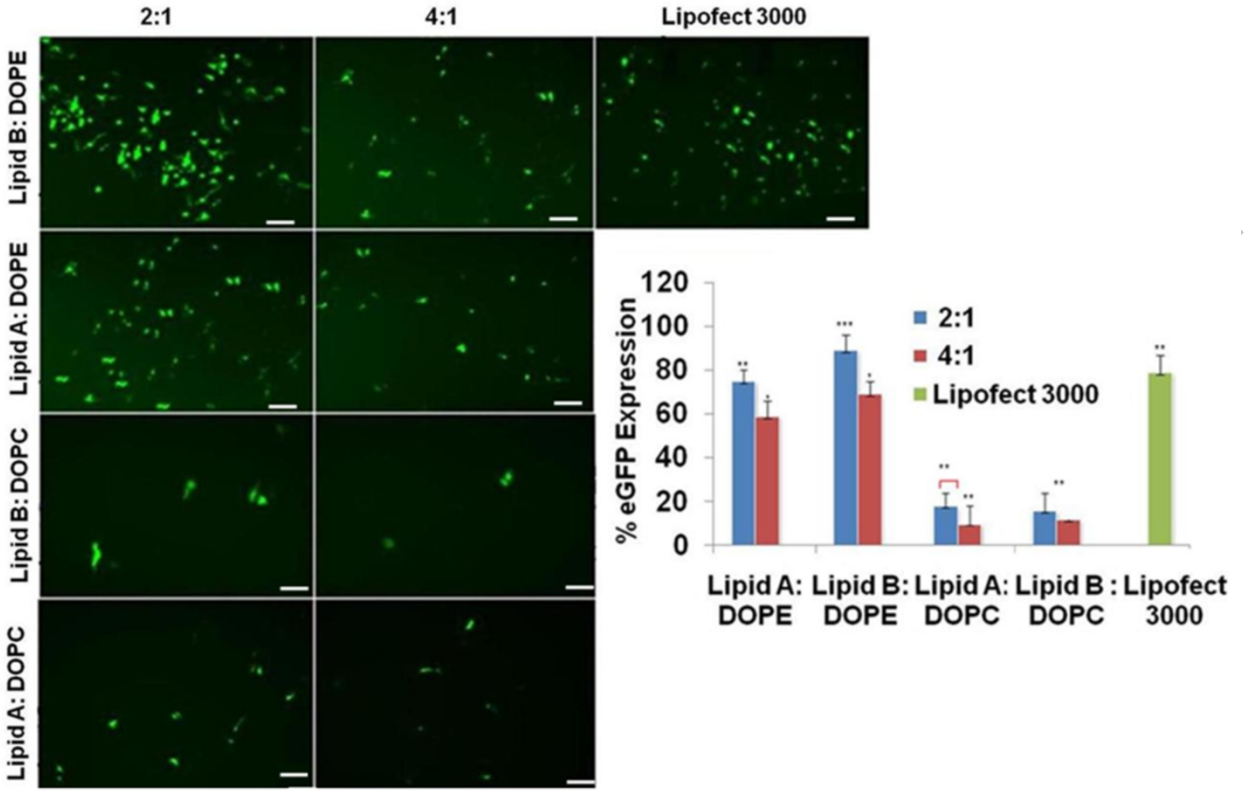

Figure 6. Transient transfection in HepG2cells using plasmid DNA pEGFP :A) Representative fluorescence images depicting GFP expression DNA at charge ratios 2:1 and 4:1.Lipoplexes with either DOPE or DOPC (1:2) was prepared. Cells were treated and incubated for 4 h in presence of 10% serum later changed to complete media and incubated for 48 h. Images were acquired 48 h post transfection). Representative graph depicts the transfection efficiencies in terms of percentage GFP positive cells. Statistical analysis was performed by Two-way ANOVA (*P<0.05, **P<0.01, ***P<0.001). (Magnification/scale Bars = 100 μm)

Cellular uptake study of Lipid A & Lipid B:

As transfection efficiencies are directly linked to the extent of internalization, we then monitored uptake behavior of lipoplexes prepared with **Lipid A: DOPE, Lipid B**: **DOPE**, **Lipid A: DOPC** and **Lipid B: DOPC** in both TCHO (CHO-5-HT_{1A}R) and CHO cells. Cells were incubated with lipoplexes labeled with Rhodamine-PE and complexed with *p*CMV-β-gal plasmid at 2:1 charge ratio for 4 h. Following uptake, cells displaying fluorescence were analyzed and quantified. It was observed that fluorescence was maximal in

TCHO cells with **Lipid B: DOPE** (**Figure 7),** following the rank order: **Lipid B: DOPE** > **LipidA**: **DOPE** > **LipidB**: **DOPC** > **LipidA: DOPC.** We believe that particle sizes of lipoplexes may play a vital role in facilitating cell uptake. This is evident from data obtained with **Lipid B: DOPE** where the size at 2:1, being the lowest, may contribute to its high activity. The other reason for these observations is the presence of the β-hydroxyl linker functionality in its spacer region in **Lipid B** that may promote hydrogen bonding interactions with the serotonin receptor [36-40] leading to higher transfection

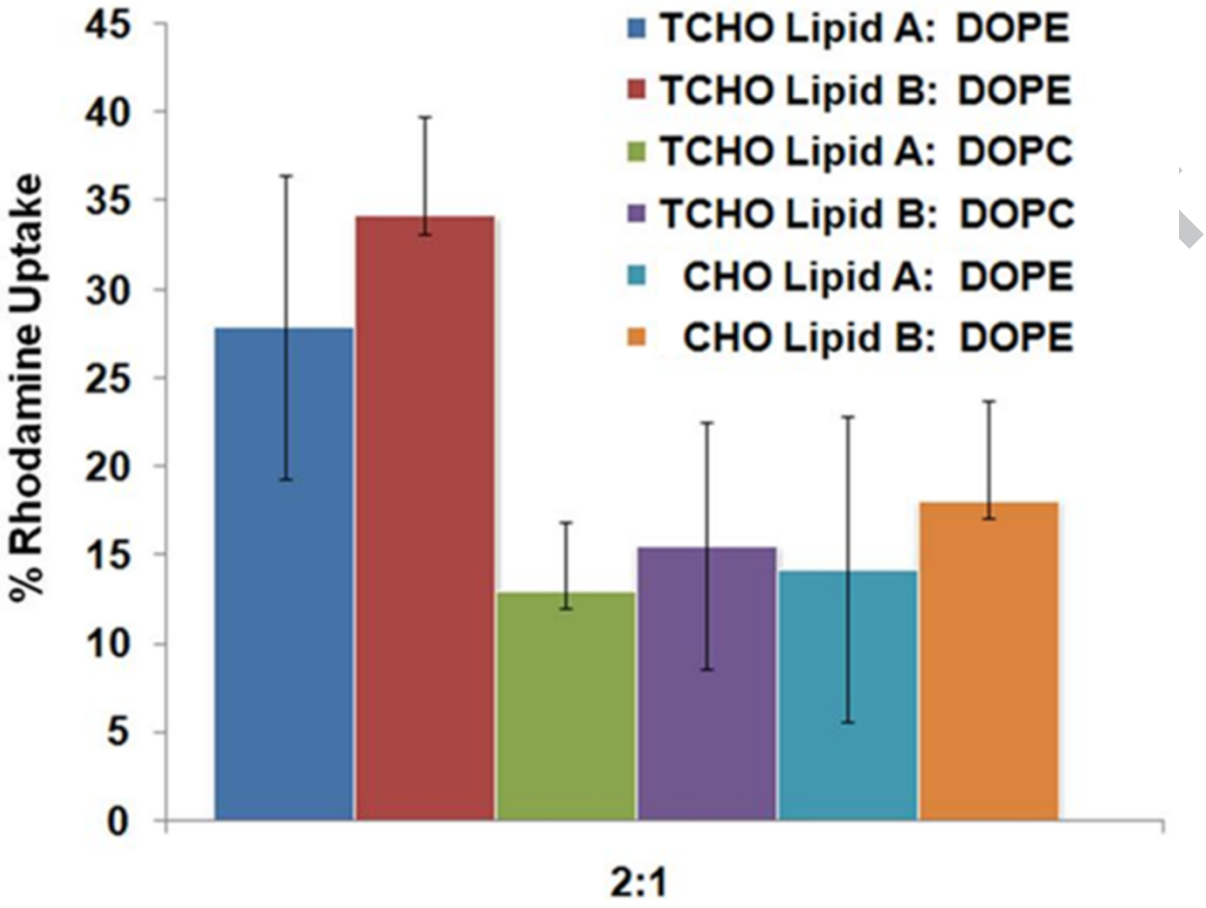

Figure7. Quantitative uptake of rhodamine-labeled lipoplexes prepared with **Lipid A** and **Lipid B** formulated with DOPE and DOPC using pCMV-β-gal plasmid DNA at 2:1 charge ratio in TCHO & CHO cells. Cells were incubated for 4h following measurement of rhodamine uptake by flow cytometry. Statistical analysis was performed by Two-way ANOVA ($P<0.005$). The details of the experiments are as described in the text.

Effect of serum on transfection mediated by Lipid A and Lipid B

One of the major drawbacks of cationic lipids, being positively charged, is the lack of stability in serum which hinders its use in *in-vivo*. This is believed to be due to the fact that transfection activity of cationic lipids decreases drastically upon interaction of negatively charged serum proteins eventually hampering the efficient interaction with cell surface leading to reduced internalization of lipoplexes [41, 42]. Hence, there is a need to develop strategies that foster the stability of lipoplexes in serum. Unfortunately, the details of lipoplex-serum interactions are still

poorly understood. In order to investigate stability of the conjugates under study, **Lipid A** and **Lipid B** formulations, were evaluated in the presence of increasing amounts of serum in CHO, TCHO, HepG2 and Neuro- 2a cells. Reporter gene expression assays, in the presence of serum with lipids formulated with DOPE led to enhancement in transfection efficiency. In contrast, formulations with either **Lipid A** or **Lipid B** with **DOPC**, the activity was drastically reduced (**Figure 8**). We surmise that negatively charged serum proteins upon interaction within lipoplexes prepared with DOPE may alter the morphology favorably following aggregation of lipoplexes. Moreover, size-dependent uptake of lipoplexes and the increase in transfection efficiency in serum may arise due to the serum-induced switch from a clathrin- dependent to a caveolae-mediated mechanism of lipoplex internalization [43].

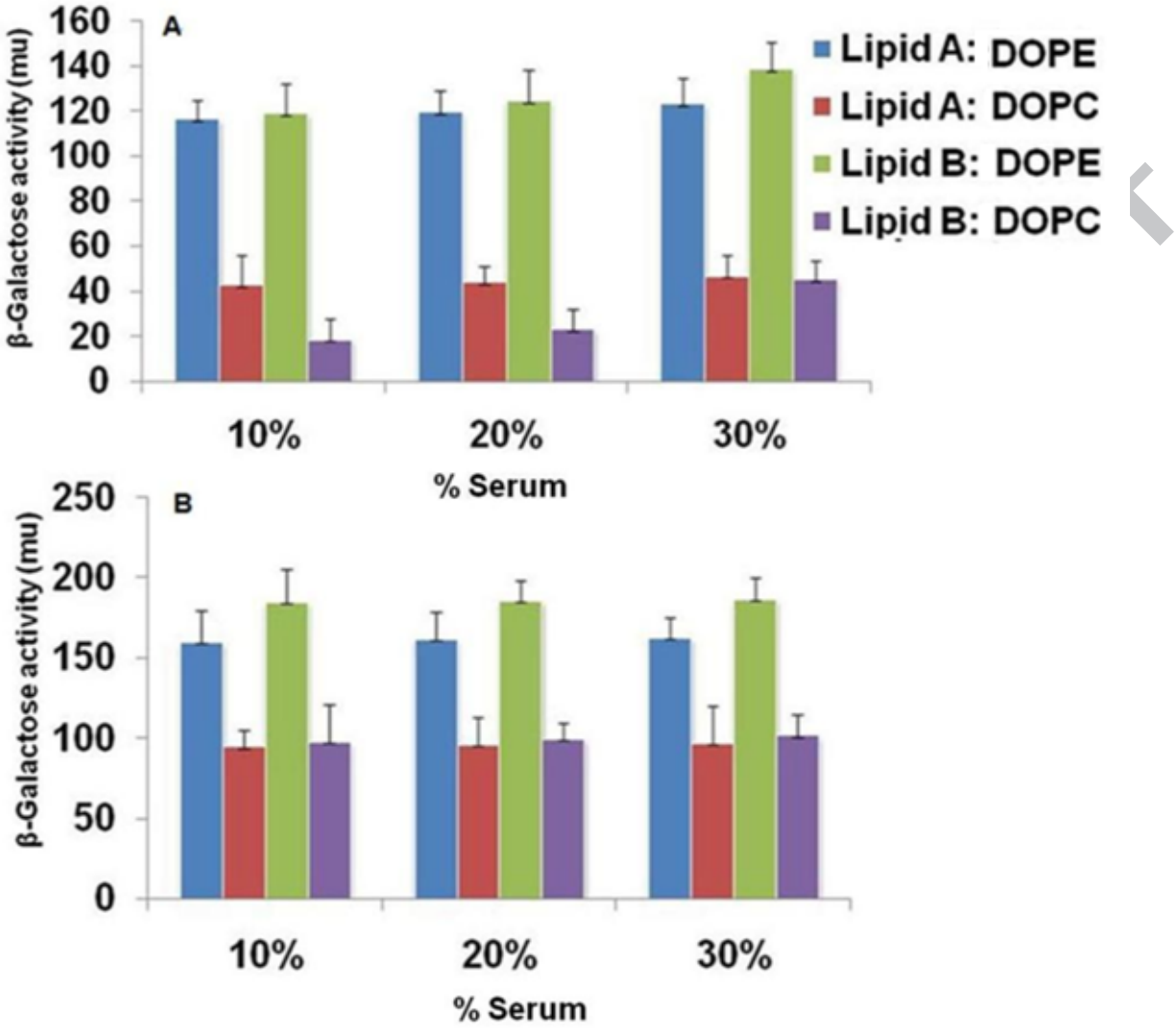

Figure 8.Transfection in the presence of serum. Lipoplexes prepared with **Lipid A and Lipid B** in the presence of increasing concentrations of serum in (A) CHO (B) and TCHO. *In vitro* transfection efficiencies of formulations prepared using pCMV-b- Gal at charge ratio of 2:1. The error bar indicates that the standard error. The difference in the data obtained is statistically significant in all charge ratios ($P < 0.003$).

Intracellular trafficking

Poor intracellular trafficking is often associated with limitations such as size and hydrophilic nature of formulations that affect the transfection efficiency. Also, size of lipoplexes having a direct bearing on internalization and affects transfection by impeding movement across the

plasma. Friend and Labat-Moleur et al. established endocytosis as the major mechanism [44] for the cellular entry of non-viral vectors. Following endocytosis, internalized lipoplexes tend to be trapped in intracellular vesicles that eventually fuse with lysosomes and are degraded [44] (Ballyetal, 1999). To overcome these problems, strategies that circumvent clathrin-mediated endocytosis can be used to deliver DNA [43, 45] (Dokka and Rojanasakul, 2000). Our observations encouraged us to explore this aspect by evaluating their entry mechanisms using various inhibitors, **Figure 9.** Towards probing the internalization mechanism of lipoplexes prepared with **Lipid A** and **Lipid B**, cells were pre-treated with inhibitors namely chlorpromazine (Braeckmans K and Vercauteren D, 2010), a clathrin pathway inhibitor, filipin-III, a caveolae pathway inhibitor and m-β-cyclodextrin, cholesterol depletion /clathrin and caveolae path way inhibitor prior to transfection with **Lipid A** and **Lipid B** formulations. Gene expression results clearly indicate uptake of lipoplexes occurs predominantly *via* clathrin path way (**Figure 11**).

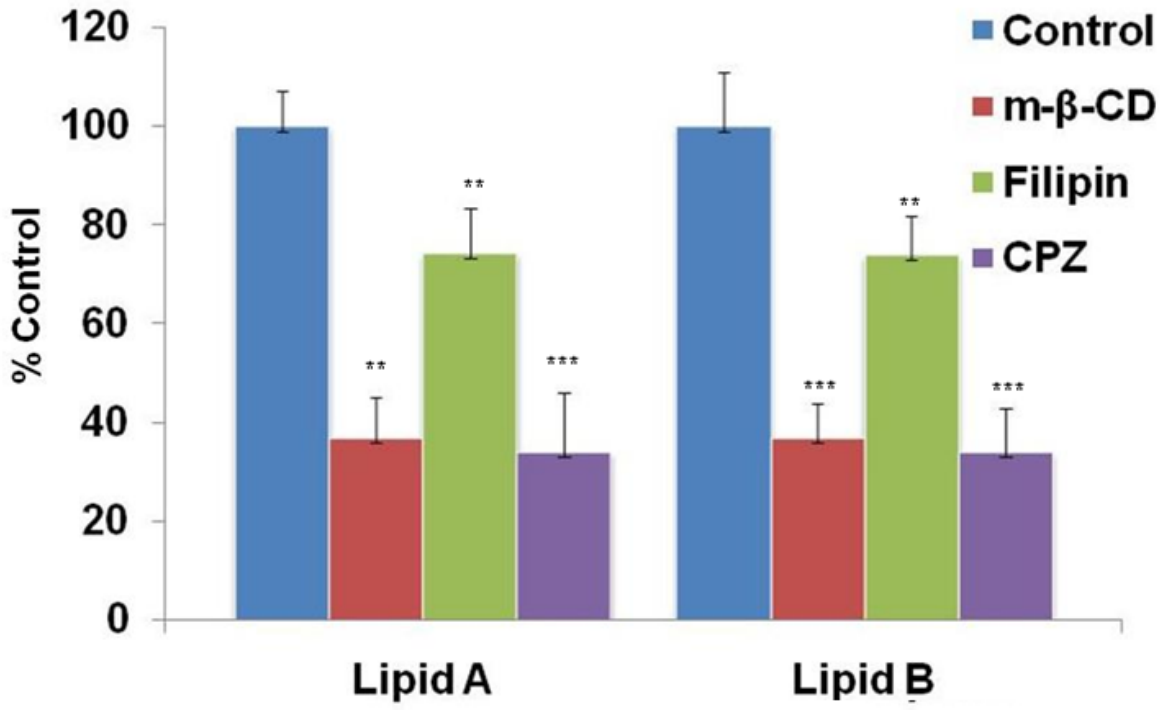

Figure. 9. Transfection using pEGFP plasmid (0.8 μg/well) in HepG2 cell line in the presence of endocytosis inhibitors: Normalized % of GFP +ve cells were obtained from GFP fluorescent

quantification of three individual experiments 48 h of post transfection. Cells were pretreated with the inhibitors (control: sky blue), methyl-β-cyclodextrin (m-β-CD, 10 μg mL^{-1}orange), Filipin-III (5μgmL^{-1} blue) and chlorpromazine (CPZ,10 μgmL^{-1}green) for 1 h prior to lipoplex addition. Cells and incubated for further 4 h after treatment with lipoplexes. Statistical analysis was performed by Two-way ANOVA (**P<0.01,***P<0.001).

Evaluation of ROS levels:

Cancer cells constantly generate high levels of reactive oxygen species (ROS) leading to non-specific damage of protein and consequent cell death. Moreover, ROS level can induce lipid peroxidation and disrupt the membrane lipid bilayer structure that inactivate the membrane-bound receptors. In addition, cationic lipids are known to induce ROS levels [46, 47] that could trigger the necroptosis cascade. The diverse pharmacological properties of α-tocopherol and their anti- oxidant properties have been established. Along with, the indole amine derivatives, serotonin possesses strong antioxidant and radical scavenging activity. In combination with surface active phospholipids such as DOPC and DOPE may induce cooperative antioxidant potential through the regeneration of tocopheryloxyl radical [48]. To examine this property, we conducted a fluorescence-based assay using HEK- 293T cells and dichlorofluorescin diacetate (DCFDA) as the fluorescent probe and tested the ability of **Lipid A** and **Lipid B** in ROS quenching. N-acetyl cysteine (NAC), a powerful antioxidant was taken as a negative control. Piperlongumine, a ROS inducer and enhancer of ROS levels, was used as a positive control. Lipoplex formulations of **Lipid B: DOPE** induced maximum ROS quenching at 2:1 charge ratio when compared to **Lipid B**: **DOPC, Lipid A**: **DOPE** and **Lipid A: DOPC** complexes at 2:1 charge ratio, **Figure 10**. The greater ROS quenching potential of **Lipid B** formulated with DOPE is not surprising as the primary amine head group of DOPE but not DOPC, increased the anti-oxidant activity of alpha-tocopherol by regeneration of the alpha-tocopherol quinone. Besides, antioxidant and membrane binding properties of serotonin protect lipids from

oxidation. This indicates that the quenching, which relies on the size of the lipoplex, may compromise cellular uptake of lipoplexes, there by resulting in reduced activity. In comparison, the functional **Lipid A: DOPE** and **Lipid A: DOPC** complexes showed a moderate decrease in the ROS levels which substantiates the efficient ROS quenching attribute of **Lipid B**: **DOPE**.

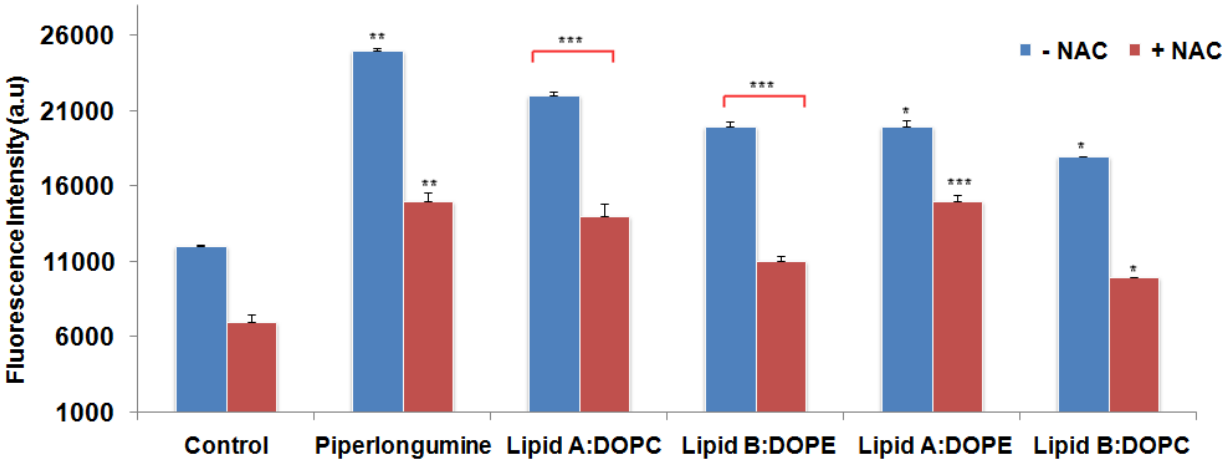

Figure.10. ROS Assay in HEK293T cells following treatment with liposomal formulations by flow cytometry. *In vitro* ROS measurement was carried using DCFDA fluorescence assay. Statistical analysis was performed by Two-way ANOVA (*P<0.05, **P<0.01,***P<0.001).

Toxicity studies

Cell viability being a major limiting factor for biological applications, we next evaluated the toxicity of **Lipid A** and **Lipid B**. This is with the anticipation that the conjugate will retain the potent anti-oxidant properties while reducing the toxicity, leading to an increase in cell viability upon transfection in vitro. CHO, TCHO, HepG2, HEK-293T and Neuro-2a cells were plated as described in the methods and then examined using MTT (**Figure11**). This was followed by further incubation in serum for 48h. As seen in **Figure 12, more** than 85% cells were viable at charge ratio 4:1. At higher charge ratio 8:1, > 70% of cells were viable (**Figure 11**), which indicates that difference observed in the transfection assays are unlikely to originate from lipid toxicity and that the α-tocopherol-serotonin hybrid based formulations, when compared to Lipofectamine 3000, are non-toxic. The presence of biodegradable carbonate and β-hydroxy

based linker group may have further contributed to reduction in toxicity and transfection efficiency compared to Lipofectamine 3000.

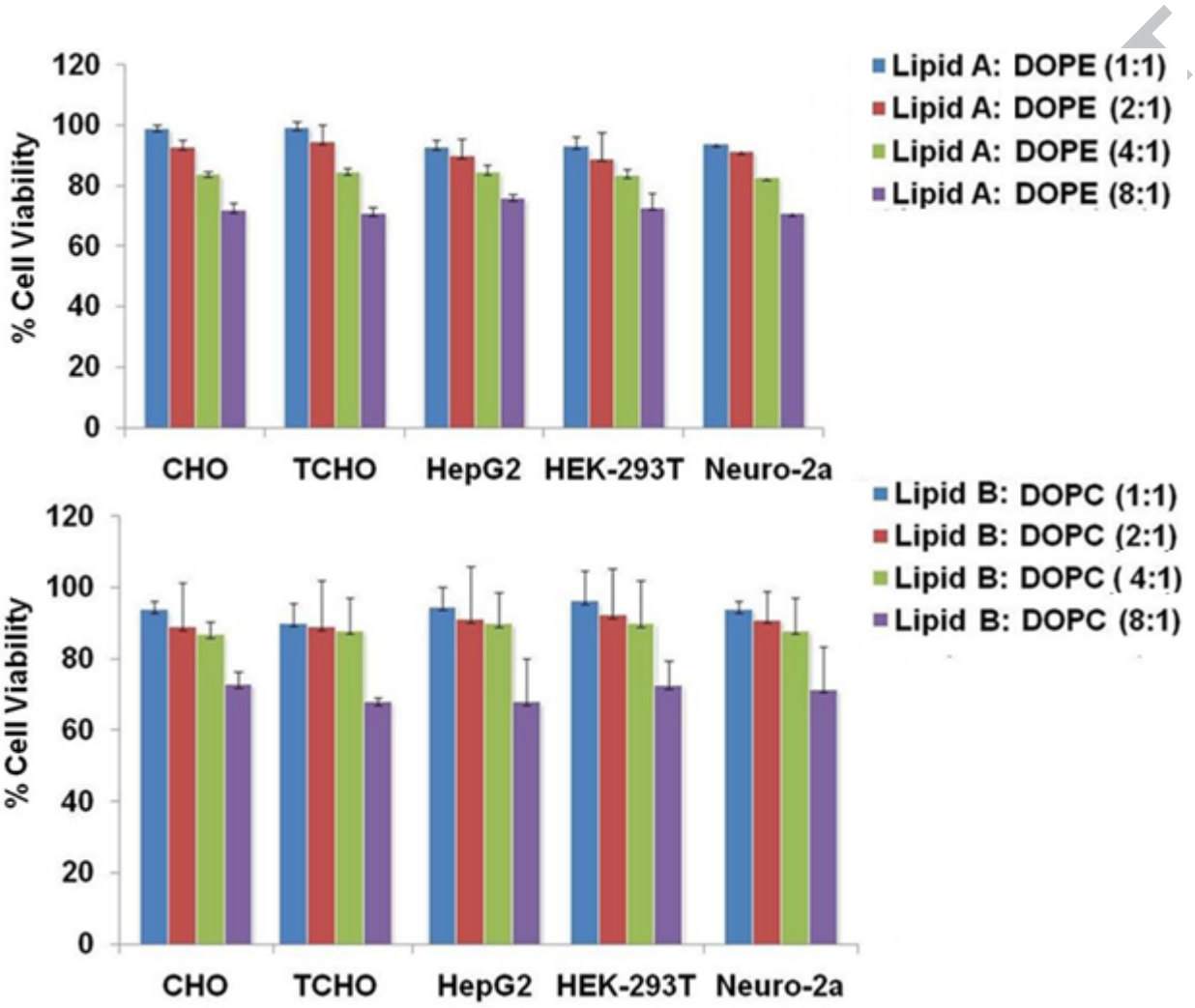

Figure 11. Tetrazolium-based colorimetric assay (MTT assay). Graph represents % viability of cells treated with **Lipid A** (A) and **Lipid B** formulations (B) Lipoplexes were prepared using the plasmid DNA (0.3 μg/well) across the charge ratios ranging from 2:1 to 8:1. The data obtained is the average values of three independent experiments (n=3). Statistical analysis was performed by Two-way ANOVA ($P<0.001$).

Molecular Docking studies

Having demonstrated the potential of **Lipid A** and **Lipid B** to mediate receptor-specific gene transfection, we then examined the binding mode of the lipids to the endogenous

neurotransmitter serotonin through molecular docking studies *in silico*. Also, lack of structural in formation of serotonin1A receptor (5-HT_{1A}) [49] motivated us to evaluate the binding geometry of the conjugates upon interaction with the corresponding receptor, however using well-known available structures of serotonin and 5-HT_{1B} receptor [50] that has 39% sequence similarity with that of 5-HT_{1A} **(Figure 13**). This was implemented in Maestro (version9.2, Schrödinger, LLC, New York, NY, 2011) and the most favorable binding conformations of the docked complex from these analyses were selected. Glide scores obtained from these studies as depicted in **Table 1**, enable the estimation of binding affinity of the ligand conjugated to **Lipid A** and **Lipid B** with the receptor[51].

Table1: Glide scores obtained through docking studies

Compound	**Glide score (kcal/mole)**
Serotonin	-5.7
Lipid A	-10.9
Lipid B	-4.9

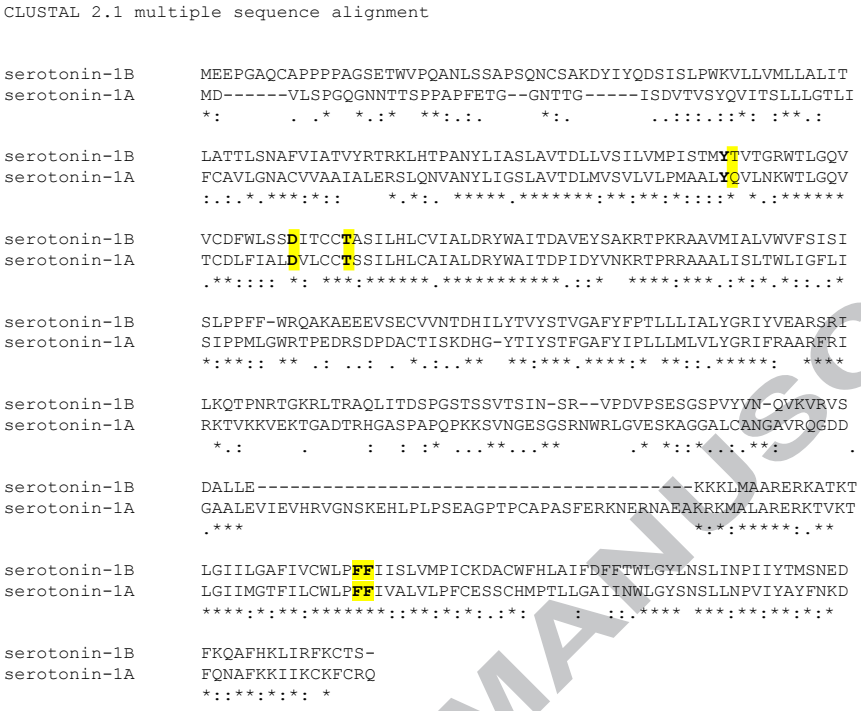

Figure 12. Sequence alignment of serotonin-1A receptor with serotonin-1B receptor shows good similarity in the transmembrane regions of the two receptors. These are the regions which contain the conserved residues Y109, D129, T134, F331 and F332, involved in the binding of serotonin. A structural alignment of serotonin-1B (PDB id: 4IAR) and a model structure of serotonin-1A shows a good superposition of the two structures in the transmembrane regions, with an RMSD of 3.03A^{o}.

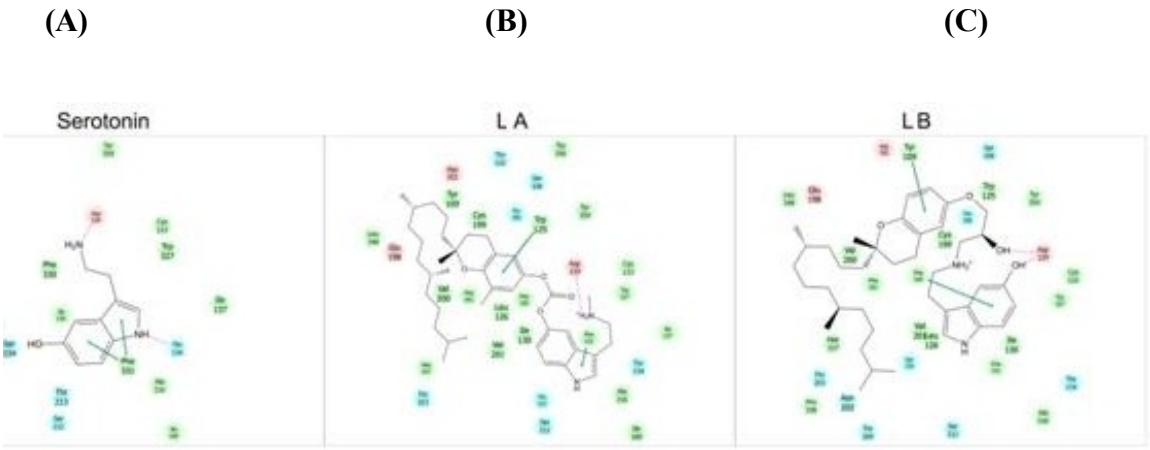

Figure 13. 2D Ligand-receptor interaction diagram of A) Serotonin, B) **Lipid A** and C) **Lipid B** making optimal interactions with serotonin receptor. The dotted lines indicate hydrogen bond interactions and solid lines indicate π-π stacking interactions.

Studies reveal that **Lipid A** exhibits greater affinity to serotonin receptor than **Lipid B, Table 1.** Interestingly, the **Lipid B** and serotonin having similar G scores suggest similar binding affinity. Additionally, interaction of the ligand to the active site on the receptor is conserved and where Asp129, Thr134 and Phe331 were shown to interact with serotonin as reported earlier [50][29] **Figure 12** and **Figure 13**. The indole ring of serotonin molecule displays π-π stacking interactions with Phe 331 and N-H of pyrrole, there is hydrogen bonding with Thr134 and free-NH_2 group with Asp 129 (**Figure 13A**). Pyrrole ring in **Lipid A** was shown to have π-π stacking interactions with Phe331and fused tetrahydropyran with Trp125 along with hydrogen bond interactions of free amino ethyl group with Asp 129 (**Figure 13B**). Phenyl group of indole ring in **Lipid B** was shown to have π-π stacking interactions with Phe 330 and fused tetrahydropyran with Tyr 109 and 5-hydroxyl group of indole and hydroxyl group in linker was shown to have hydrogen bond interactions with Asp129 (**Figure 13C**).The involvement of hydroxyl group of serotonin moiety may favor hydrogen bonding interactions with the receptor, in accordance with the reported mutational and modeling studies [52, 53]where $serotonin_{1A}$ receptor prefers ligands with hydrogen bond acceptor at a position

corresponding to the hydroxyl group in serotonin. The docking studies similarly show that **Lipid B** with the free hydroxyl group is available for interaction with serotonin$_{1A}$ receptor, (**Figure 13)**. The present study also offers a unique insight into how a differentially tethered serotonin head group to the lipid tocopherol affects the overall receptor binding and efficiency, signifying that higher G scores may not be an indicator of biological activity observed. Here, the differential conjugation of serotonin to tocopherol enables the formulation of two different lipids similar in all structural components but differing in the functional moiety freely present in the distal end of the head group. The significance is that the activity differences between **Lipid A** and **B** could be directly linked to the presence of either amino or hydroxy terminal or their subsequent interactions with the 5-HT1a receptor promoting sequential adhesion, endocytosis and transfection. Earlier agonist binding studies of 5-HT1a receptor indicated the involvement of ion-pair formation between the protonated amino group as well as the hydroxyl group of serotonin with the aspartate or serine/threonine residues of the 5-HT1a receptor respectively[54] which sheds light on the significance of both the functional group in serotonin-receptor interactions. However when formulated with the co-lipid DOPE, multiple parameters determine the receptor binding affinity such as the liposomal surface structural reorganization (liposome-ligand length from receptor), flexibility of the tethered ligand to overcome the hydrodynamic drag force of the solvent on the liposome, receptor segregation induced by ligand adhesion and plasma membrane deformation induced by curvature of the respective liposomes[55]. Comparative transfection studies of the formulations showed greater activity in the cells examined except in HEK293T. These findings suggest the involvement of phenolic hydroxyl group of serotonin moiety in the hydrogen bonding interactions with the receptor. This is also in accordance with earlier mutational studies wherein the involvement of reactive hydroxyl was first demonstrated[54] by Ho et al. 1992. Subsequent mutational studies together with molecular modeling also demonstrated preference of serotonin$_{1A}$ receptor to ligands corresponding to hydroxyl group in serotonin [55] (Style et al 1996 and Kuipers et al 1997).

Taking cues from these studies, in a different approach, Gopal et al., covalently conjugated serotonin to DSPE- PEG – 2000 to the amino group to reconstitute formulations to mediate selective targeting[34] (Gopaletal.2011). In this study, computational simulations of serotonin, reported here provide insights into the binding mode of the ligand to the receptor. The modeling studies (**Table I**, **Figure 13 A-C**) show that free ligand serotonin and **Lipid B** with the free hydroxyl group that is available for interaction with serotonin1_A receptor prefer ligands with a hydrogen bond acceptor have similar G score predicts similar binding mode when compared to **Lipid B**. This is also validated through our experiments wherein transfection of **Lipid A** is surpassed by that of **Lipid B** influenced by co-lipid DOPE. Docking studies reveal that **Lipid A** has a higher affinity than **Lipid B**, and in vitro studies showed greater activity with **Lipid B**. It is possible that a conformational change in the receptor could arise from the differential binding orientation of the tethered ligands (**amino** vs **hydroxyl**). The results indicate that both the amino and hydroxyl tethered serotonin conjugated liposomes interacted with the same active site of 5-HT1a receptor similar to native serotonin, thus promoting transfection. Importantly, this explains the higher transfection rate of **Lipid B** and scope for further development of non- viral vectors for nucleic acid delivery to the central nervous system.

Conclusion

Our studies conclusively demonstrate the efficacy and utility of the designed and developed tocopherol formulation i.e. **Lipid B:** DOPE for targeted delivery of nucleic acids. The methodology, in principle, may be applicable for targeted delivery of nucleic acids in vitro to neuronal cells and cancer cell lines that express serotonin receptors. Additionally supported by molecular docking studies, **Lipid B** with the hydroxy functionality exhibits specific targeting with higher transfection efficiency *in vitro* and serum compatibility thus having considerable scope for the development of non-toxic tocopherol formulations for targeted *in vivo* applications.

Experimental section

General procedure and chemicals reagents

Mass spectral data were acquired by using a commercial LCQ ion trap mass spectro-meter (Thermo Finnigan, SanJose, CA, U.S.) equipped with an ESI source.^{1}H NMR and ^{13}C NMR spectra were recorded on a Varian FT400 MHz NMR spectrometer. Serotonin and α-Tocopherol was purchased from Sigma Co. Super negatively charged eGFP plasmid, and rhodamine-PE were ample gifts from IICT (Indian Institute of Chemical Technology, Hyderabad, India). Lipofectamine-3000 was purchased from Invitrogen Life Technologies, polyethylene glycol 8000, and o-nitrophenyl-β-D-galactopyranoside (pDNA) were purchased from Sigma (St. Louis, MO, U.S.). NP-40, antibiotics, and agarose were purchased from Hi-media, India. 1,2-dioleoyl-*sn*-glycero-3-phosphoethanolamine (DOPE) and DOPC were purchased from Fluka (Switzerland). Unless otherwise stated, various organic solvents including, pyridine, triethylamine, methanol, methylene chloride (DCM), phosphomolybdic acid spray reagent, epichlorohydrin, and potassium hydroxide (KOH) were purchased from Sigma-Aldrich Co. and were used without further purification. The progress of the reaction was monitored by thin-layer chromatography using 0.25 mm silica gel plates. Column chromatography technique was executed with silica gel (Acme Synthetic Chemicals, India; finer than 200 and 60-120 mesh). Elemental analyses were performed by High Resolution Mass Spectrometry (HRMS) using QExactive equipment (Thermo Scientific) and purity of lipids were characterised by HPLC (Shimadzu LC Solution) and showed more than 95% purity. HepG2, CHO, Neuro-2a and HEK-293T cells were procured from the National Centre for Cell Sciences (NCCS), Pune, India. Cell were grown at 37 ˚C in Dulbecco's modified Eagle's medium (DMEM) with 10% FBS in humidified atmosphere containing 5% CO2 / 95 % air.

Synthesis of tert-butyl (2-(5-hydroxy-1H-indol-3-yl) ethyl) carbonate from serotonin (1, Scheme 1)

1.0 g of serotonin hydrochloride (4.7 mmol) in dry methanol solution was taken in a flame-dried Schlenk flask under an argon atmosphere. To this triethyl amine (1.51 mL, 10.3 mmol) was added and the solution is cooled to 0°C. Boc_2O (1.54g, 7.05 mmol) dissolved in methanol was added drop wise to the above solution. After 3 h of stirring, the resulting mixture was quenched with water, transferred to a separation funnel, and extracted three times with DCM. The combined organic phases were dried (Na_2SO_4), filtered under suction, and concentrated in

vacuum. The product was purified by column chromatography (EtOAc / pentane 1:1) and isolated as a yellow solid (1.21 g, 4.38 mmol, 93%).

^{1}H NMR (400 MHz, $CDCl_3$) : δ 8.05 (s, 1H), 7.25 (d, J = 8.8, 1H), 7.06 (d, J = 1.8, 1H), 7.00 (s, 1H), 6.90 (dd, J = 2.4, 8.8, 1H), 6.33−5.96 (m, 1H), 5.45 (dq, J = 1.6, 17.3, 1H), 5.29 (dq,J = 1.4, 10.5, 1H), 4.65 (brs, 1H), 4.59 (dt, J = 1.4, 5.3, 2H), 3.63−3.30 (m, 2H), 2.91 (t, J =6.5, 2H), 1.44 (s, 9H).^{13}C NMR(100 MHz, CDCl3): δ 156. 2, 152. 7, 133. 9, 131. 8, 127. 6, 123. 1, 117.3, 112.6, 112.3, 112.0, 102.2, 79.2, 69.9, 40.9, 28.4, 25.7. ESI Mass m/z: - 299.

Synthesis of Tocopherylchloroformate from Tocopherol (2, Scheme 1)

To a 250 mL of round bottom flask 1g of (+/_)-α-tocopherol in 10 mL dry THF, 0.2 mL of NEt_3 was added, stirred for 10 minutes and then 0.5 mL of diphosgene in dry THF was added drop wise with pressure equalizing funnel about 30 minutes at 0 ˚C. The reaction mixture was stirred overnight. Charcoal was added to reaction mixture, stirred for 10 minutes and then filtered. The solvent was removed under rotary evaporator. The residue was purified with column by using 60-120 mesh size silicagel. The compound was eluted by hexane. The yield of the compound was 90%. (Rf: 0.7 TLC; Hexane).

^{1}H NMR (400 MHz, $CDCl_3$): δ 9.4 [s, 1H-indole], 7.6 [s, 1H, -imidazole=CH], 7.4 [s, 1H-aromatic], 7.2 [d, 1H-aromatic], 7.4 [d, 1H-aromatic], 7.8 [s, 1 CO-NH amide-broad], 1.8(s, 9H– $C(CH_3)_3$, 2.9 [t, 2H], 2.8[t, 2H], 0.8-0.9 [m, 12H, CH-CH_3tocopheryl], 1.00-1.4 [m, 18H, -$(CH_2)_9$ tocopheryl], 1.7-1.8 [[m, 2H, CH2-3 tocopheryl], 2.05 [s, 3H, CH3-5 tocopheryl], 2.15 [m, 9H, tocopheryl], 2.18 [s, 3H, CH3-7 tocopheryl], 2.55-2.6 [t, 2H, CH2-4 tocopheryl] ppm. ESI m/z: -755

^{1}H NMR (400 MHz, $CDCl_3$): δ 0.8-0.9 [m, 12H, CH-CH_3 tocopheryl], 1.00-1.4 [m, 18H, -$(CH_2)_9$ tocopheryl], 1.7-1.8 [[m, 2H, CH2-3 tocopheryl], 2.05 [s, 3H, CH3-5 tocopheryl], 2.15 [s, 3H, CH3-8tocopheryl], 2.18 [s, 3H, CH3-7 tocopheryl], 2.55-2.6 [t, 2H, CH2-4 tocopheryl] ppm. ESI Mass m/z: 492+NH_4=510.

***O*-Acylation of BOC-Protected Serotonin with Tocopherylchloroformate (3, Scheme 1)**

To 0.5g (1mmol) of tocopherylchloroformate dissolved in dry DCM in100 mL round bottom flask added triethyl amine (0.5 mmol). The above mixture was added drop wise about 20 minutes to tert-Butyl (2-(5-hydroxy-1H-indol-3-yl) ethyl) carbonate (1.1 mmol) with the help of pressure equalizing funnel. The reaction mixture was stirred for 12 h at room temperature. The resulting mixture was quenched with 2N HCl and water, transferred to a separation funnel, and extracted three times with DCM. The combined organic phases were dried (Na_2SO_4),

filtered and concentrated in vacuum. The product was purified by column (Rf: - 0.3 in 10% EtOAc/ hexane). The product yield is 95%.

^{1}HNMR (400 MHz, $CDCl_3$): δ 9.4[s, 1H-indole], 7.6[s, 1H, -imidazole=CH], 7.4 [s, 1H-aromatic], 7.2 [d, 1H-aromatic], 7.4 [d, 1H-aromatic], 7.8 [s, 1 CO-NH amide-broad], 1.8 (s, 9H–$C(CH_3)_3$, 2.9 [t, 2H], 2.8 [t, 2H], 0.8-0.9 [m, 12H, CH-CH_3 tocopheryl], 1.00-1.4 [m, 18H,-$(CH_2)_9$ tocopheryl], 1.7-1.8 [[m, 2H, CH2-3 tocopheryl], 2.05 [s, 3H, CH3-5 tocopheryl], 2.15 [m, 9H, tocopheryl], 2.18 [s, 3H, CH3-7 tocopheryl], 2.55-2.6 [t, 2H, CH2-4 tocopheryl] ppm. ESI m/z: -755.

Deprotection of BOC Protected Serotonin lipid (4, Scheme 1)

0.1 g of Boc-serotonin tocopherylchloroformate was dissolved in 5 mL of dry DCM in 100 mL Round bottom flask under inert atmosphere. To this solution 0.05 mL of TFA was added. The reaction mixture was stirred for 12 h at room temperature. The resulting mixture was concentrated in vacuum about 20 min for removing excess TFA. The residue was purified by column chromatography (100-200 size silica gel) (Rf: - 0.1 in 10% Methanol/ chloroform v/v). The product of yield is 95%.

^{1}HNMR (400 MHz, $CDCl_3$): δ 9.4 [s, 1H-indole], 7.6 [s,1H,-imidazole=CH], 7.4 [s, 1H-aromatic], 7.2 [d, 1H-aromatic], 7.4 [d, 1H-aromatic], 7.8 [s, 1CO-NHamide-broad], 2.8 [t, 2H], 0.8-0.9 [m, 12H, CH-CH_3tocopheryl], 1.00-1.4 [m, 18H, -$(CH_2)_9$ tocopheryl], 1.7-1.8 [[m, 2H, CH2-3tocopheryl], 2.05 [s, 3H, CH3-5tocopheryl], 2.15[m, 9H, tocopheryl], 2.18 [s, 3H, CH3-7 tocopheryl], 2.55-2.6 [t, 2H, CH2-4 tocopheryl] ppm.

^{13}C NMR (100 MHz, $CDCl_3$) δ 154.17, 153.74, 149.72, 144.46, 144.26, 141.08, 139.30,134.43,133.28,129.31,126.80,126.72,126.00,125.43,125.08,124.01,123.51,123.28,117.69,115,91,115.21,114.41,114.11,113.97,112.34,110.06,109.60,109.30,107.68,75.23,55.99,40.22,39.75,39.40,37.59,37.49,37.44,37.32,34.75,33.87,32.82,32.73,31.97,31.65,31.00,30.20,29.95,29.74,29.59,29.41,29.20,28.99,28.01,24.85,24.49,23.67,22.76,22.66,21.06, 20.52, 19.78, 19.71, 14.17, 12.77, 11.91, 11.81.

HRMS (ES) m/z: - calculated 633.46302, found. 633.46256., HPLC: purity 95%

Synthesis of epoxidation of alpha tocopherol with Epichlorohydrine (5, Scheme 2)

To a stirred mixture of (+/_)-α-tocopherol (5.42 g, 12.58 mmol), rac-epichlorohydrin (1.74 g, 18.87 mmol), and tetra-butyl ammonium hydrogensulfate 0.43g, 1.13 mmol) at 0°C, added 50% KOH solution (3.24 g, 57. 8 mmol) in water (6.5 mL). The reaction mixture was warmed to room

temperature and stirred for 4h, extracted with Et_2O, washed with water, dried with anhydrous Na_2SO_4, filtered, and concentrated under reduced pressure. The crude product was purified by silica gel column chromatography to give α-tocopherylglycidyl ether 1 (5.89 g, 12.10 mmol, 89 %) as a clear oil. The yield of compound was 96%.Rf=0.69 (EtOAc/hexane).

^{1}H,NMR (400MHz, $CDCl_3$): δ 0.84 (d, J= 6.4 Hz, 3H), 0.85 (d, J=6.4 Hz, 3H), 0.87 (d, J=6.4Hz, 6H), 1.00–1.60 (m, 21H), 1.23 (s, 3H), 1.71–1.85 (m, 2H), 2.08 (s, 3H), 2.14 (s, 3H), 2.18 (s, 3H), 2.57 (t, J = 6.8 Hz, 2 H), 2.70 (dd, J = 5.0, 2.6 Hz, 1 H), 2.87 (dd, J = 5.0, 4.0 Hz, 1H), 3.35 (dddd, J = 5.8, 4.0, 3.2, 2.6 Hz, 1 H), 3.66 (ddd, J = 11.0, 5.8, 1.8 Hz, 1H),3.90 (ddd, J = 11.0, 3.2, 1.6 Hz, 1 H) ppm. ESI Mass m/z :(486+1) =487.

Synthesis of regioselective epoxide ring opening (α-tocopheryl glycidyl ether) with Serotonin (6, Scheme 2)

To a solution of serotonin in (1.85 g, 0.01 mol) 2 mL of dry pyridine was added and stirred at −10 °C for 1 h. A solution of alphatocopheryl glycidyl ether (1.9 g, 0.01 mol) in 1 mL of methylene chloride (DCM) was cooled to –10 °C and was added drop-wise to the above mixture about 30min. After 12 h of stirring at-10°C, the reaction mixture was diluted with 20 mL of toluene and concentrated in vacuo. The residue was purified with60-120 mesh silica gel. The compound was eluted by 4% Chloroform in Methanol. The yield of the compound was 70% (Rf: 0.3 TLC; 3-4% Chloroform in Methanol)

NMR (400 MHz, DMSO) δ/ppm 10.6 [s, indole NH], 8.6 [s, imidazole =CH], 7.2 [d,1H aromatic],6.8 [d, 1H-aromatic], 6.9 [s, 1H-aromatic], 5.8 [m, 1H CH_2-COH_2-CH_2], 5.0 [d, 2H], 4.6 [d, 2H], 4.1 [2H, broad-CH_2-NH,-CH_2OH-CH_2], 2.8 [t, 2H-NH-CH_2-CH_2-], 3.3 [t,2H], 0.8-0.9 [m, 12H, CH-CH_3 tocopheryl], 1.00-1.4 [m, 18H, -$(CH_2)_9$ tocopheryl], 1.7-1.8 [m, 2H, CH2-3tocopheryl], 2.05 [s, 3H, CH3-5 tocopheryl], 2.15 [s, 3H, CH3-8 tocopheryl], 2.18 [s, 3H, CH3-7 tocopheryl], 2.55-2.6 [t, 2H, CH2-4 tocopheryl] ppm.

^{13}C NMR (100 MHz, $CDCl_3$) δ 207.06, 149.82, 148.03, 146.82, 131.25, 127.46, 127.32,125.62,124.01,122.80,117.53,114.07,112.28,108.58,100.43,85.55,78.12,77.92,74.80,66.09,40.54,39.38,37.45,37.30,33.83,32.80,31.93,30.93,29.70,29.52,29.37,29.17,28.96,27.98,24.81,24.48,23.43,22.73,22.64,21.07,20.52,19.76,19.69,14.12,12.55,11.70.

HRMS (ES) m/z: calculated 662.45687 found: 663.

Quaternization of Serotonin Lipid B. (7, Scheme 2)

To a stirred solution of the tertiary serotonin α-tocopherol in dry methanol, excess anhydrous HCl was added. The reaction mixture was stirred for 12 h at room temperature. The residue was concentrated under vacuum. The crude product was purified by column chromatography (MeOH: $CHCl_3$ 1:9 v/v) to afford the quaternized α-tocopherol-serotonin lipid as a yellow color.

^{1}H NMR (400 MHz, DMSO) δ/ppm 10.6 [s, indole NH], 8.6 [s, imidazole =CH], 7.2 [d, 1H aromatic], 6.8 [d, 1H-aromatic], 6.9 [s, 1H-aromatic], 5.8 [m, 1H CH_2-COH_2-CH_2], 5.0 [d, 2H], 4.6 [d, 2H], 4.1 [2H, broad-CH_2-NH,-CH_2OH-CH_2], 2.8 [t, 2H-NH-CH_2-CH_2-], 3.3 [t,2H], 0.8-0.9 [m, 12H, CH-CH_3tocopheryl], 1.00-1.4 [m, 18H, -$(CH_2)_9$tocopheryl], 1.7-1.8 [[m, 2H, CH2-3 tocopheryl], 2.05 [s, 3H, CH3-5 tocopheryl], 2.15 [s, 3H, CH3-8 tocopheryl], 2.18 [s, 3H, CH3-7 tocopheryl], 2.55-2.6 [t, 2H, CH2-4 tocopheryl] ppm.
^{13}C NMR (100 MHz, $CDCl_3$) δ 207.06, 149.82, 148.03, 146.82, 131.25, 127.46, 127.32, 125.62, 124.01, 122.80, 117.53, 114.07, 112.28, 108.58, 100.43, 85.55, 78.12, 77.92, 74.80, 66.09, 40.54, 39.38, 37.45, 37.30, 33.83, 32.80, 31.93, 30.93, 29.70, 29.52, 29.37, 29.17, 28.96, 27.98, 24.81, 24.48, 23.43, 22.73, 22.64, 21.07, 20.52, 19.76, 19.69, 14.12, 12.55, 11.70.
HRMS (ES) m/z: calculated 663.45687 found: 663.50954. , HPLC: 96% purity.

DNA binding assay:

To elucidate the DNA binding capability of liposomes with Lipid: DNA, lipoplexes were prepared at charge ratios ranging from 1:1 to 8:1 using 0.3 μg plasmid DNA in a total volume of 30 μL in HEPES buffer (pH 7.4) and further incubated at room temperature for 20-25 minutes. 4 μL of 6x loading buffer (0.25% Bromophenol blue in 40% (w/v) sucrose with sterile H_2O) was added to it and from the resulting solution 30 μL was loaded on each well. The samples were electrophoresed at 80 V for 45 minutes and the agarosegel (pertained with EtBr) was imaged following visualization using a Bio-Rad Gel Doc XR+ imaging system (Bio-Rad, Hercules, CA, USA) and analyzed.

Heparin Displacement Assay

Heparin was used to study the anionic displacement of pDNA from lipoplexes. Lipid: pDNA complexes were prepared as described in the above section (pDNA binding assay) and incubated for 20 min. Following the incubation, 0.1 μg of sodium salt of heparin was added and incubated for another 30 min. Samples were electrophoresed in an agarose gel (1.5%) and pDNA bands were visualized as mentioned in the above section.

Zeta potential (ξ) and size measurements

Size and the surface charge (zeta potentials) of liposomes and lipoplexes with varying charge ratios (8:1 to 1:1) were measured by photon correlation spectroscopy and electrophoretic mobility on a Zetasizer3000 HSA (Malvern,U.K.). Measurements were carried out in DMEM media with a sample refractive index of 1.59 and a viscosity of 0.89 cP. The system was calibrated by using the 2005 nm polystyrene polymer (Duke Scientific Corps., Palo Alto, CA, U.S.). The diameters of liposomes and lipoplexes were calculated by using the automatic method. Zeta potential was also measured using the following parameters: viscosity, 0.89 cP; dielectricconstant,79; temperature, 25 °C; F(Ka), 1.50 (Smoluchowski); maximum voltage of the current, V. The system was calibrated by using DTS0050 standard from Malvern. Measurements were done 10 times with the zero-field correction. All the liposomes and lipoplexes of the size measurements were done 10 times in triplicate with the zero field correction and values represented as the average of triplicate measurements. The potentials were measured 10 times and represented as their average values calculated by using the Smoluchowski approximation.

Cytotoxicity (MTT) assay (Mitochondrial activity)

The MTT (3-(4,5-dimethylthiazol-2-yl)-2, 5-diphenyltetrazolium Bromide) based reduction cytotoxicity assays of **Lipid A & B** were carried out in CHO, Neuro-2a, HEK-293T, and HepG2 cells across the lipid:DNA charge ratios of 1:1-8:1 in 96-wells plate. Briefly, 24 h after adding lipoplexes, MTT (0.5 mg/mL in DMEM) was added to cells and incubated for 4 h at 37 $^{\circ}$C. Results were expressed as percent viability = [A540 (treated cells)-background/A540 (untreated cells)-background] x100.

Transfection Biology:

CHO, TCHO, Neuro-2a, HEK-293T, and HepG2 cells were seeded at a density of 10,000 per well, in a 96-well plate, 18-24 h before transfection. Then 0.3 µg (0.91 nmol) of plasmid DNA was complexed with different concentrations of liposomal formulations of **Lipid A** and **B** i.e. 1:1 to 8:1 in DMEM medium (total volume made up to 100 µL) for 30 min. Just prior to transfection, cells plated in the 96-well plate were washed twice with PBS (100 µL) followed by the addition of lipoplexes (lipid-DNA complexes). After 4 h of incubation, 100 µL of DMEM with 20% FBS was added to the cells. The medium was replaced with 10% complete medium after 24 h, and reporter gene activity was estimated after 48 h. Cells were washed twice with PBS (100 µL each) and lysed in 50 µL lysis buffer [0.25 M Tris-HCl (pH 8.0) and 0.5% NP40]. The β-galactosidase activity per well was estimated by adding 50 µLof 2 substrate

solution [1.33 mg/mL ONPG, 0.2 M sodium phosphate (pH 7.3), and 2 mM magnesium chloride] to the lysate. Absorbance of the product ortho-nitrophenol at 405 nm was converted to β-galactosidase units by using a calibration curve constructed using pure commercial β-galactosidase enzyme. Each transfection experiment was repeated 3 times on 3 different days. The transfection values were noted as an average of three replicate transfection plates, performed on three different days. The values of β-galactosidase units in replicate plates assayed on the same day varied by less than 20%.

ROS assay

Intracellular ROS generation was measured by 2', 7'–dichlorofluorescindiacetate (DCF-DA) method given by Kim *et al.*, 2010 with slight modifications. HEK-293 cells were seeded into a 24 well plate 12 h before the transfections. After 24 h of the treatment with the liposome/p DNA, the cells were incubated with 10 μM DCF-DA at 37 °C for 15 min. Qualitative cellular fluorescence images were captured by fluorescence microscopy by exiting at 488 nm and emitting at 525 nm (Leica DMI6000B inverted Microscope).

Treatment with inhibitors: Cells were incubated with chlorpromazine (CPZ, 10 μg mL−1), filipin-III (5 μg mL−1) and methyl-β-cyclodextrin (m-β-CD, 10 mg mL−1) (all from Sigma) in normal cell culture medium for 1 h at 37 °C prior to the addition of lipoplexes formulated with **Lipid A** and **B**. Consequently, cells were incubated for 4 h, trypsinized and collected in 10% FBS containing PBS, followed by analysis using FACS. The concentration of chlorpromazine (CPZ) employed in the study were such that uptake of fluorescently labeled lipoplexes of **Lipids A** and **B**, which is widely recognized as a ligand exclusively internalized via clathrin-independent endocytosis, was inhibited by 80–95 % , since it has been reported that this lipoplexes is exclusively internalized via a clathrin-independent mechanism.

Cellular eGFP Expression Study.

For cellular α5GFP expression experiments in HEK-293T and HepG2, 50,000 cells were cultured in 24-wells plate, 18-24 h before transfection. Then 0.9 μg of eGFP plasmid DNA encoding green fluorescent protein was complexed with liposomes of **Lipids A** & **B** at charge ratio (lipid/DNA) 2:1 in DMEM medium (total volume made up to 100 μL) for 30 min. Just prior to transfection, cells plated in the 24-wells plate were washed with PBS (2×100 μL) followed by addition of lipoplexes. The media 400 μL was added after 4 h incubation of the

cells. After 24 h, the complete medium was removed, and cells were washed with PBS (2×200 µl). Finally, 200 µL of PBS was added to each per well cells and visualized under the epifluorescence microscope to observe green fluorescent protein.

Serum stability

Cells were plated at a density of 15,000 cells (HEK-293T and CHO) per well in a 96-well plate, 18-24 h prior to transfection. Then 0.3 µg (0.91 nmol) of eGFP was complexed with **Lipid A** & **B** in DMEM medium in the presence of varying serum (10-30% v/v and total volume made up to 100 µL) for 30 min. The charge ratios of lipid/eGFP plasmid were maintained at 2:1, at which the two lipids exhibited their highest transfection ability in four different types of viz. HepG2, Neuro-2a, HEK-293T, CHO and TCHO (TCHO-$5HT_{1A}$R). TCHO stably expresses the human $serotonin_{1A}$ receptor compared to CHO cells. The experimental procedure and determination of eGFP activity per well are similar to that reported for the *in-vitro* transfection experiments.

Statistical analysis:

The results were expressed as (mean standard deviation). Statistical importance between treatments was assessed by the ANOVA test followed by the Dennett multiple comparison test (*p<0.05, **P<0.01,***P<0.001).

Cellular Uptake

Cells were cultured at a density of 10 000 cells/ well in a 96-well plate 16−24 h prior to treatment in 200 μL of growth medium until cells are 30−50% confluent at the time of transfection. pDNA (0.3 μg of pDNA diluted to 50 μL with serum-free DMEM media) was complexed with rhodamine-PE labeled cationic liposomes (diluted to 50 μL with DMEM) of lipids **A** and **B** using 2:1 lipid to pDNA charge ratio. The cells were washed with PBS (1×200 μL) and then treated with lipoplexes, and incubated in a humidified chamber containing 5% CO_2 at 37 °C. After a 4 h incubation period, cells were washed with PBS (3×200 μL) to remove the dye and fixed with 3.8% paraformaldehyde in PBS at room temperature for 10 min. The cell displaying fluorescence were analyzed and quantified using flow cytometry (BD Biosciences, San Jose, CA, USA) with BDFACS Celesta Software (BD Biosciences).

Docking studies

Preparation of Ligands: The ligands were built using ChemBiodraw 13.0 and were saved as MOL file. The ligands were loaded into Maestro 9.2 software and optimized using LigPrep tool. The possible ionization states at pH 7 ± 2 were generated using OPLS2005 force field. Single conformation with lowest potential energy for each minimized compound was retained for further docking.

Preparation of the receptor protein: The crystal structure of 5-HT_{1B} (PDBid:4IAR) having bound ergotamine to the active site Asp129 was taken for the study. The protein structure was prepared using Protein Preparation Wizard tool. The missing side chains were added to the structure using Schrödinger Prime 3.0 (Prime version 3.0, Schrödinger, LLC, New York, NY, 2011). Hydrogen's were added and water molecules were deleted within 5 A^o from the crystal chain. The entire process was adjusted to a pH range of 7.0 ± 4. The optimization was performed to a maximum root mean square deviation (RMSD) of 0.3 A^o using OPLS2005 force field.

GRID generation: The receptor grid was generated with dimensions (10 x 10 x 10 A^o). The resultant GRID file was used for docking.

Docking: The receptor GRID was selected using Ligand Docking tool and docking was set in XP (extra precision). The minimized ligands were imported for docking to the grid selected. Epik state penalties were added to docking score and XP descriptor file was generated (.xpdes). The resultant docking study was visualized in XP visualizer.

Acknowledgement

This work was supported by the Department of Science and Technology, SERB-DST, Government of India, New Delhi, India for financial support. Venkanna thanks CSIR for a senior research fellowship. The authors thank the Tissue Culture facility at CSIR-CCMB and Vellore Institute of Technology, Vellore where cell-based assays were carried out. We acknowledge Prof. Amitabha Chattopadhyay for providing serotonin-overexpressing TCHO cell line for the study.

References

[1] M. Ramamoorth, A. Narvekar, Non viral vectors in gene therapy- an overview, Journal of clinical and diagnostic research : JCDR, 9 (2015) GE01-06.

[2] M.A. Kay, State-of-the-art gene-based therapies: the road ahead, Nature reviews. Genetics, 12 (2011) 316-328.

[3] J. Pahle, W. Walther, Vectors and strategies for nonviral cancer gene therapy, Expert opinion on biological therapy, 16 (2016) 443-461.

[4] B. Schwartz, M.A. Ivanov, B. Pitard, V. Escriou, R. Rangara, G. Byk, P. Wils, J. Crouzet, D. Scherman, Synthetic DNA-compacting peptides derived from human sequence enhance cationic lipid-mediated gene transfer in vitro and in vivo, Gene therapy, 6 (1999) 282-292.

[5] M.G. Katz, A.S. Fargnoli, R.D. Williams, C.R. Bridges, Gene therapy delivery systems for enhancing viral and nonviral vectors for cardiac diseases: current concepts and future applications, Human gene therapy, 24 (2013) 914-927.

[6] N. Nayerossadat, T. Maedeh, P.A. Ali, Viral and nonviral delivery systems for gene delivery, Advanced biomedical research, 1 (2012) 27.

[7] P. Boisguerin, S. Deshayes, M.J. Gait, L. O'Donovan, C. Godfrey, C.A. Betts, M.J. Wood, B. Lebleu, Delivery of therapeutic oligonucleotides with cell penetrating peptides, Advanced drug delivery reviews, 87 (2015) 52-67.

[8] G. Dorraj, J.J. Carreras, H. Nunez, I. Abushammala, A. Melero, Lipid Nanoparticles as Potential Gene Therapeutic Delivery Systems for Oral Administration, Current gene therapy, 17 (2017) 89-104.

[9] L. Zhu, V.P. Torchilin, Stimulus-responsive nanopreparations for tumor targeting, Integrative biology : quantitative biosciences from nano to macro, 5 (2013) 96-107.

[10] L. Zhang, P. Zhang, Q. Zhao, Y. Zhang, L. Cao, Y. Luan, Doxorubicin-loaded polypeptide nanorods based on electrostatic interactions for cancer therapy, Journal of colloid and interface

science, 464 (2016) 126-136.

[11] Y. Jiang, F. Li, Y. Luan, W. Cao, X. Ji, L. Zhao, L. Zhang, Z. Li, Formation of drug/surfactant catanionic vesicles and their application in sustained drug release, International journal of pharmaceutics, 436 (2012) 806-814.

[12] R.A. Schwendener, Liposomes as vaccine delivery systems: a review of the recent advances, Therapeutic advances in vaccines, 2 (2014) 159-182.

[13] G. Sahay, D.Y. Alakhova, A.V. Kabanov, Endocytosis of nanomedicines, Journal of controlled release : official journal of the Controlled Release Society, 145 (2010) 182-195.

[14] T.A. Wynn, T.R. Ramalingam, Mechanisms of fibrosis: therapeutic translation for fibrotic disease, Nature medicine, 18 (2012) 1028-1040.

[15] P.M. Lembo, M.H. Ghahremani, P.R. Albert, Receptor selectivity of the cloned opossum G protein-coupled receptor kinase 2 (GRK2) in intact opossum kidney cells: role in desensitization of endogenous alpha2C-adrenergic but not serotonin 1B receptors, Mol Endocrinol, 13 (1999) 138-147.

[16] P.R. Albert, Transcriptional regulation of the 5-HT1A receptor: implications for mental illness, Philosophical transactions of the Royal Society of London. Series B, Biological sciences, 367 (2012) 2402-2415.

[17] O. Stiedl, E. Pappa, A. Konradsson-Geuken, S.O. Ogren, The role of the serotonin receptor subtypes 5-HT1A and 5-HT7 and its interaction in emotional learning and memory, Frontiers in pharmacology, 6 (2015) 162.

[18] B. Yameen, W.I. Choi, C. Vilos, A. Swami, J. Shi, O.C. Farokhzad, Insight into nanoparticle cellular uptake and intracellular targeting, Journal of controlled release : official journal of the Controlled Release Society, 190 (2014) 485-499.

[19] G. Bozzuto, A. Molinari, Liposomes as nanomedical devices, International journal of nanomedicine, 10 (2015) 975-999.

[20] N. Gurbuz, A.A. Ashour, S.N. Alpay, B. Ozpolat, Down-regulation of 5-HT1B and 5-HT1D receptors inhibits proliferation, clonogenicity and invasion of human pancreatic cancer cells, PloS one, 9 (2014) e110067.

[21] N. Dizeyi, A. Bjartell, E. Nilsson, J. Hansson, V. Gadaleanu, N. Cross, P.A. Abrahamsson, Expression of serotonin receptors and role of serotonin in human prostate cancer tissue and cell lines, The Prostate, 59 (2004) 328-336.

[22] S. Azouzi, H. Santuz, S. Morandat, C. Pereira, F. Cote, O. Hermine, K. El Kirat, Y. Colin, C. Le Van Kim, C. Etchebest, P. Amireault, Antioxidant and Membrane Binding Properties of Serotonin Protect Lipids from Oxidation, Biophysical journal, 112 (2017) 1863-1873.

[23] S. Rizvi, S.T. Raza, F. Ahmed, A. Ahmad, S. Abbas, F. Mahdi, The role of vitamin e in human health and some diseases, Sultan Qaboos University medical journal, 14 (2014) e157-165.
[24] B.J. Boucher, W.B. Grant, H.P. Bhattoa, Exploring the Role of Vitamin D. Comments on Fleury et al. Sun Exposure and Its Effects on Human Health: Mechanisms through Which Sun Exposure Could Reduce the Risk of Developing Obesity and Cardiometabolic Dysfunction. Int. J. Environ. Res. Public Health 2016, 13, 999, International journal of environmental research and public health, 13 (2016).
[25] J.W. Beulens, S.L. Booth, E.G. van den Heuvel, E. Stoecklin, A. Baka, C. Vermeer, The role of menaquinones (vitamin K(2)) in human health, The British journal of nutrition, 110 (2013) 1357-1368.
[26] G. Waris, H. Ahsan, Reactive oxygen species: role in the development of cancer and various chronic conditions, Journal of carcinogenesis, 5 (2006) 14.
[27] V. Muripiti, H.K. Rachamalla, R. Banerjee, S.V. Patri, alpha-Tocopherol-based cationic amphiphiles with a novel pH sensitive hybrid linker for gene delivery, Organic & biomolecular chemistry, 16 (2018) 2932-2946.
[28] P. Pires, S. Simoes, S. Nir, R. Gaspar, N. Duzgunes, M.C. Pedroso de Lima, Interaction of cationic liposomes and their DNA complexes with monocytic leukemia cells, Biochimica et biophysica acta, 1418 (1999) 71-84.
[29] M. Maccarrone, L. Dini, L. Di Marzio, A. Di Giulio, A. Rossi, G. Mossa, A. Finazzi-Agro, Interaction of DNA with cationic liposomes: ability of transfecting lentil protoplasts, Biochemical and biophysical research communications, 186 (1992) 1417-1422.
[30] F. Bordi, C. Cametti, S. Sennato, M. Diociaiuti, Direct evidence of multicompartment aggregates in polyelectrolyte-charged liposome complexes, Biophysical journal, 91 (2006) 1513-1520.
[31] M. Brgles, M. Santak, B. Halassy, D. Forcic, J. Tomasic, Influence of charge ratio of liposome/DNA complexes on their size after extrusion and transfection efficiency, International journal of nanomedicine, 7 (2012) 393-401.
[32] N. Khatri, D. Baradia, I. Vhora, M. Rathi, A. Misra, Development and characterization of siRNA lipoplexes: Effect of different lipids, in vitro evaluation in cancerous cell lines and in vivo toxicity study, AAPS PharmSciTech, 15 (2014) 1630-1643.
[33] M. Abdouh, J.M. Storring, M. Riad, Y. Paquette, P.R. Albert, E. Drobetsky, E. Kouassi, Transcriptional mechanisms for induction of 5-HT1A receptor mRNA and protein in activated B and T lymphocytes, The Journal of biological chemistry, 276 (2001) 4382-4388.
[34] J. Fantini, F.J. Barrantes, Sphingolipid/cholesterol regulation of neurotransmitter receptor

conformation and function, Biochimica et biophysica acta, 1788 (2009) 2345-2361.

[35] S. Lukasiewicz, E. Blasiak, K. Szafran-Pilch, M. Dziedzicka-Wasylewska, Dopamine D2 and serotonin 5-HT1A receptor interaction in the context of the effects of antipsychotics - in vitro studies, Journal of neurochemistry, 137 (2016) 549-560.

[36] Y. Huang, A. Thathiah, Regulation of neuronal communication by G protein-coupled receptors, FEBS letters, 589 (2015) 1607-1619.

[37] W. Yin, X.E. Zhou, D. Yang, P.W. de Waal, M. Wang, A. Dai, X. Cai, C.-Y. Huang, P. Liu, X. Wang, Y. Yin, B. Liu, Y. Zhou, J. Wang, H. Liu, M. Caffrey, K. Melcher, Y. Xu, M.-W. Wang, H.E. Xu, Y. Jiang, Crystal structure of the human 5-HT1B serotonin receptor bound to an inverse agonist, Cell discovery, 4 (2018) 12.

[38] M.V. Borroni, A.S. Valles, F.J. Barrantes, The lipid habitats of neurotransmitter receptors in brain, Biochimica et biophysica acta, 1858 (2016) 2662-2670.

[39] X.X. Zhang, T.J. McIntosh, M.W. Grinstaff, Functional lipids and lipoplexes for improved gene delivery, Biochimie, 94 (2012) 42-58.

[40] C. Corbo, R. Molinaro, A. Parodi, N.E. Toledano Furman, F. Salvatore, E. Tasciotti, The impact of nanoparticle protein corona on cytotoxicity, immunotoxicity and target drug delivery, Nanomedicine (Lond), 11 (2016) 81-100.

[41] C. Marchini, M. Montani, A. Amici, H. Amenitsch, C. Marianecci, D. Pozzi, G. Caracciolo, Structural stability and increase in size rationalize the efficiency of lipoplexes in serum, Langmuir : the ACS journal of surfaces and colloids, 25 (2009) 3013-3021.

[42] T. Nakai, T. Kanamori, S. Sando, Y. Aoyama, Remarkably size-regulated cell invasion by artificial viruses. Saccharide-dependent self-aggregation of glycoviruses and its consequences in glycoviral gene delivery, Journal of the American Chemical Society, 125 (2003) 8465-8475.

[43] I.A. Khalil, K. Kogure, H. Akita, H. Harashima, Uptake pathways and subsequent intracellular trafficking in nonviral gene delivery, Pharmacological reviews, 58 (2006) 32-45.

[44] L.M. Bareford, P.W. Swaan, Endocytic mechanisms for targeted drug delivery, Advanced drug delivery reviews, 59 (2007) 748-758.

[45] Q. Gong, C. Huntsman, D. Ma, Clathrin-independent internalization and recycling, Journal of cellular and molecular medicine, 12 (2008) 126-144.

[46] D.N. Dhanasekaran, E.P. Reddy, JNK-signaling: A multiplexing hub in programmed cell death, Genes & cancer, 8 (2017) 682-694.

[47] F.T. Andon, B. Fadeel, Programmed cell death: molecular mechanisms and implications for safety assessment of nanomaterials, Accounts of chemical research, 46 (2013) 733-742.

[48] R.H. Bisby, S. Ahmed, R.B. Cundall, E.W. Thomas, Free radical reactions with alpha-

tocopherol and N-stearoyl tryptophan methyl ester in micellar solutions, Free radical research communications, 1 (1986) 251-261.

[49] C. Wang, Y. Jiang, J. Ma, H. Wu, D. Wacker, V. Katritch, G.W. Han, W. Liu, X.P. Huang, E. Vardy, J.D. McCorvy, X. Gao, X.E. Zhou, K. Melcher, C. Zhang, F. Bai, H. Yang, L. Yang, H. Jiang, B.L. Roth, V. Cherezov, R.C. Stevens, H.E. Xu, Structural basis for molecular recognition at serotonin receptors, Science, 340 (2013) 610-614.

[50] R.A. Friesner, R.B. Murphy, M.P. Repasky, L.L. Frye, J.R. Greenwood, T.A. Halgren, P.C. Sanschagrin, D.T. Mainz, Extra precision glide: docking and scoring incorporating a model of hydrophobic enclosure for protein-ligand complexes, Journal of medicinal chemistry, 49 (2006) 6177-6196.

[51] R.X. Gu, H.I. Ingolfsson, A.H. de Vries, S.J. Marrink, D.P. Tieleman, Ganglioside-Lipid and Ganglioside-Protein Interactions Revealed by Coarse-Grained and Atomistic Molecular Dynamics Simulations, The journal of physical chemistry. B, 121 (2017) 3262-3275.

[52] S.L. Kitson, 5-hydroxytryptamine (5-HT) receptor ligands, Current pharmaceutical design, 13 (2007) 2621-2637.

[53] C.H. Cheng, B. Costall, R.J. Naylor, J.A. Rudd, The effect of 5-HT receptor ligands on the uptake of [3H]5-hydroxytryptamine into rat cortical synaptosomes, European journal of pharmacology, 239 (1993) 211-214.

[54] Z. Li, A.A. Gorfe, Receptor-mediated membrane adhesion of lipid-polymer hybrid (LPH) nanoparticles studied by dissipative particle dynamics simulations, Nanoscale, 7 (2015) 814-824.

[55] J.R. Raymond, Y.V. Mukhin, T.W. Gettys, M.N. Garnovskaya, The recombinant 5-HT1A receptor: G protein coupling and signalling pathways, British journal of pharmacology, 127 (1999) 1751-1764.